

High-Energy Emission from Spider Binaries

Alice K. Harding

Los Alamos National Laboratory

Collaborators:

Zorawar Wadiasingh,

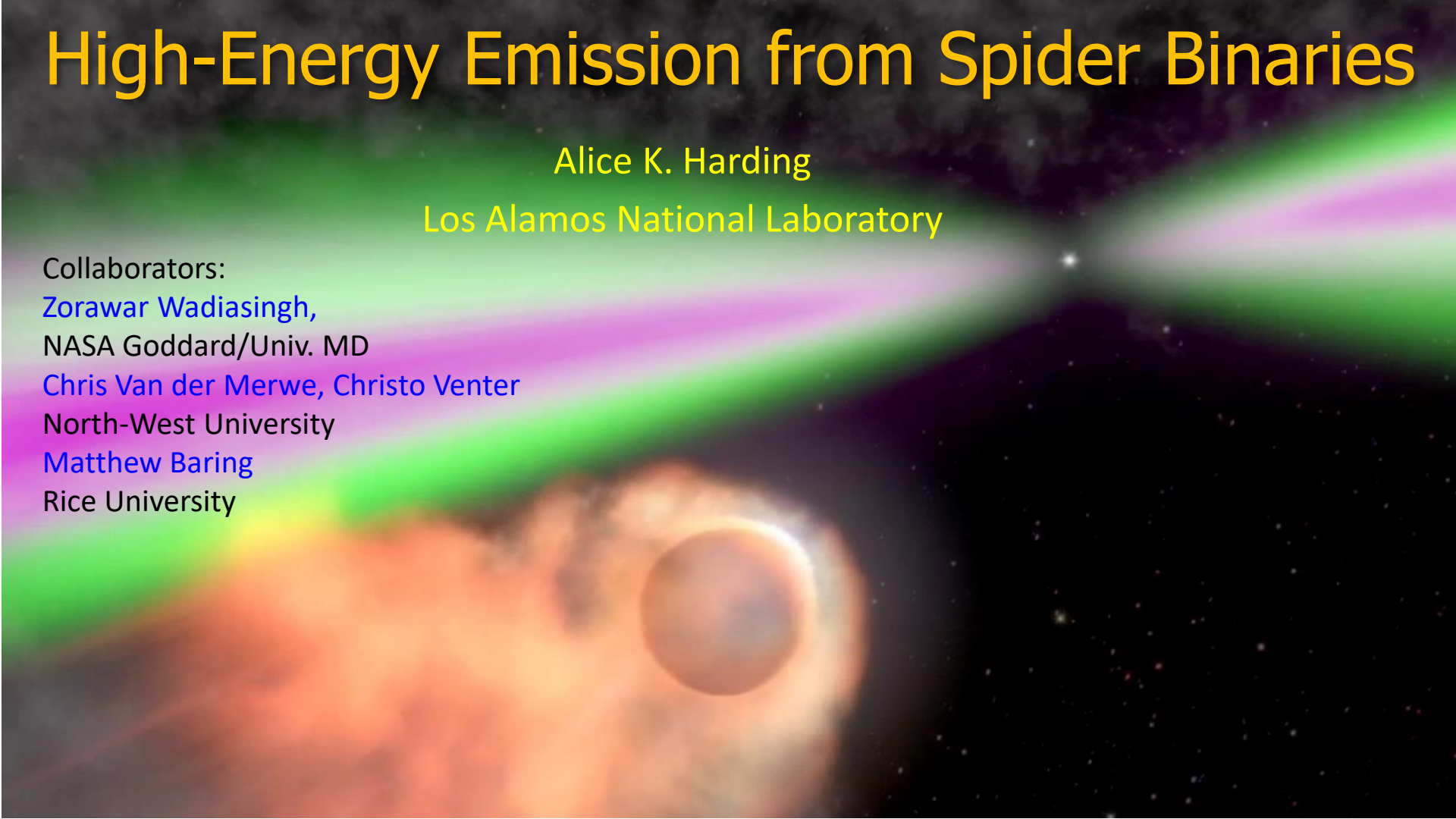
NASA Goddard/Univ. MD

Chris Van der Merwe, Christo Venter

North-West University

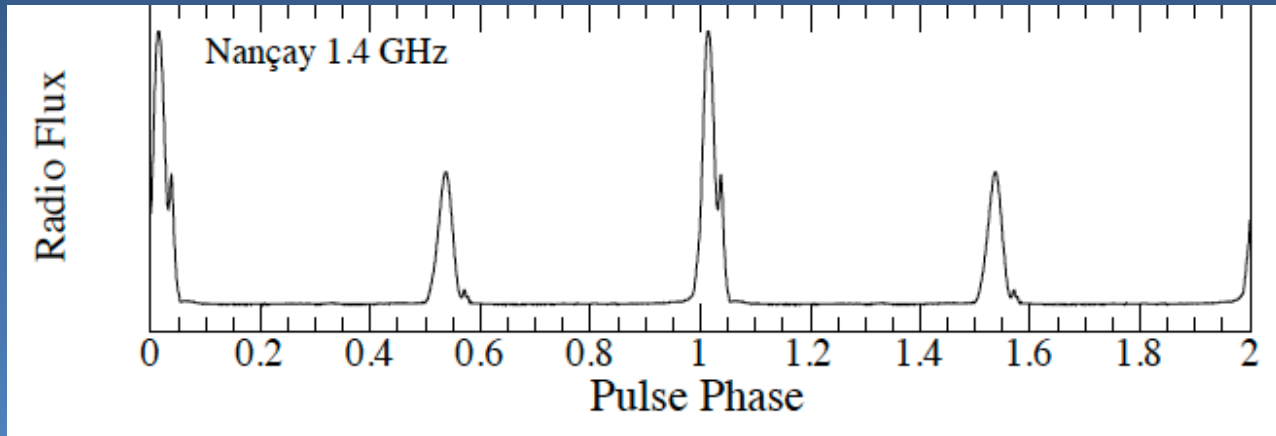
Matthew Baring

Rice University



What are millisecond pulsars?

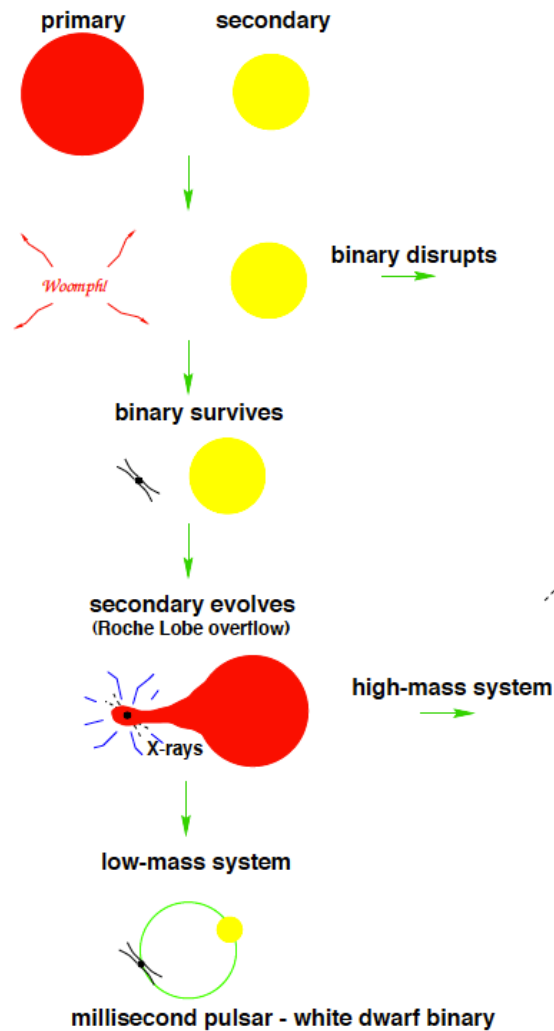
- First detected MSP – PSR J1939-2134 (Backer 1982)
 - $P = 1.558$ ms, rotation-powered
 - In binary system
 - Very low \dot{P} (and surface B_0) – but energetic, $E_{sd} = 10^{36}$ erg/s
 - Near NS break-up frequency!



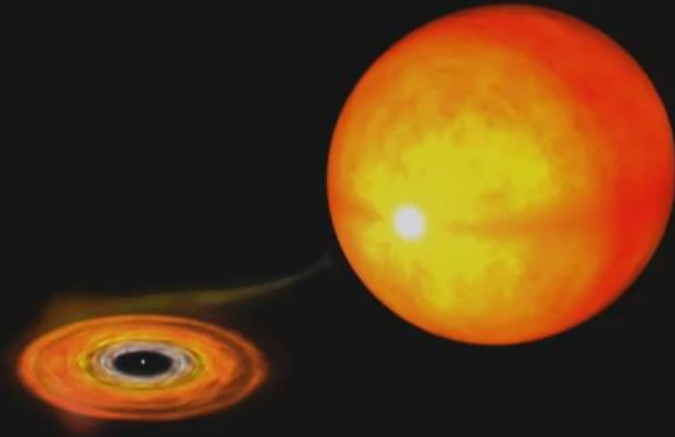
Binary spin-up model

Alpar et al. (1982)

Low-mass X-ray binary



Spin-up of a millisecond pulsar



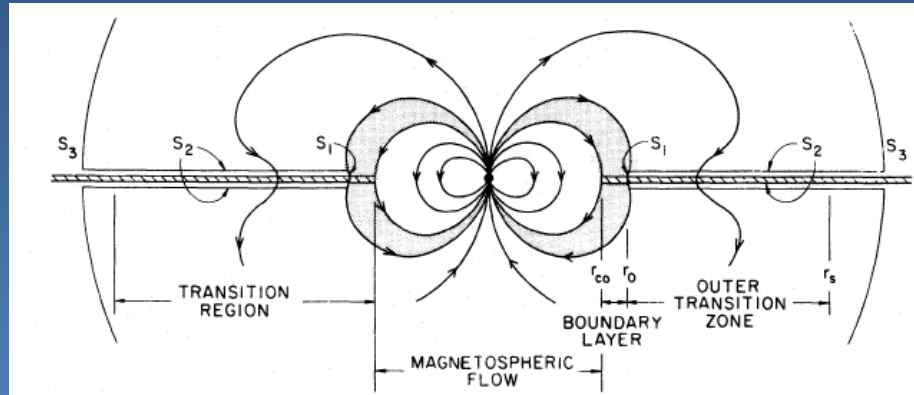
Binary spin-up model

(Davison & Ostriker 1973, Alpar et al. 1982)

Equilibrium period = Keplerian velocity at the Alfvén radius

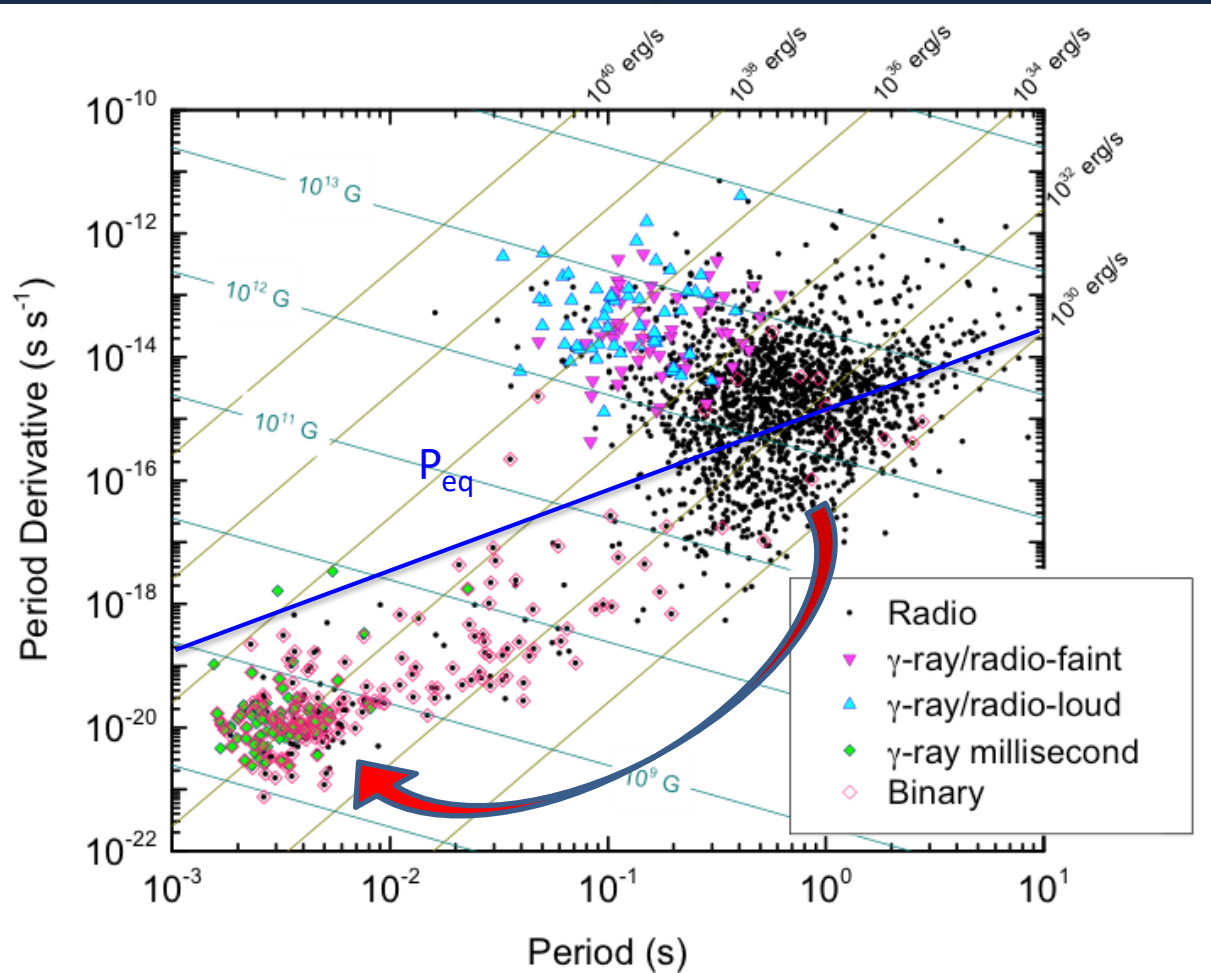
$$\Omega_{eq} = \left(\frac{GM}{R_A^3} \right)^{1/2} \quad \frac{B^2}{8\pi} = \rho v^2 \Rightarrow R_A = \left(\frac{B_0^4 R^{12}}{8GM\dot{M}_a^2} \right)^{1/7}$$

$$P_{eq} \approx 6 \times 10^4 \text{ s } B_8^{6/7} R_6^{18/7} \left(\frac{M}{M_{solar}} \right)^{-5/7} \dot{M}_{17}^{-3/7}$$



Ghosh & Lamb 1979

MSPs: recycled from the graveyard



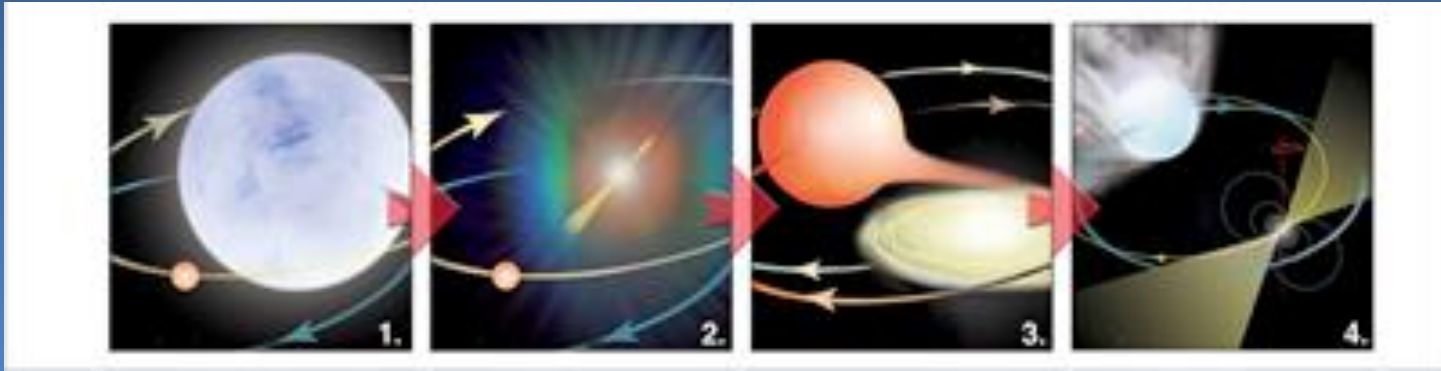
- ~ 424 field MSPs
 - $\sim 80\%$ binary
- 128 are γ -ray pulsars
- Spin periods
 - 1.5 - ~ 100 ms
- Magnetic fields $\sim 10^8 - 10^{10}$ G
- Ages $10^8 - 10^9$ yr
- “Recycled” pulsars spun-up by binary companion stars

Transitional MSPs

- **Discovery of accreting MSPs** (Wijnands & van der Klis 1998)
 - Evolutionary progenitors of radio MSPs
 - ~20 presently known: spin frequencies ~100 – 700 Hz
- **MSP accretion/spin-down in transition** (Archibald et al. 2009)

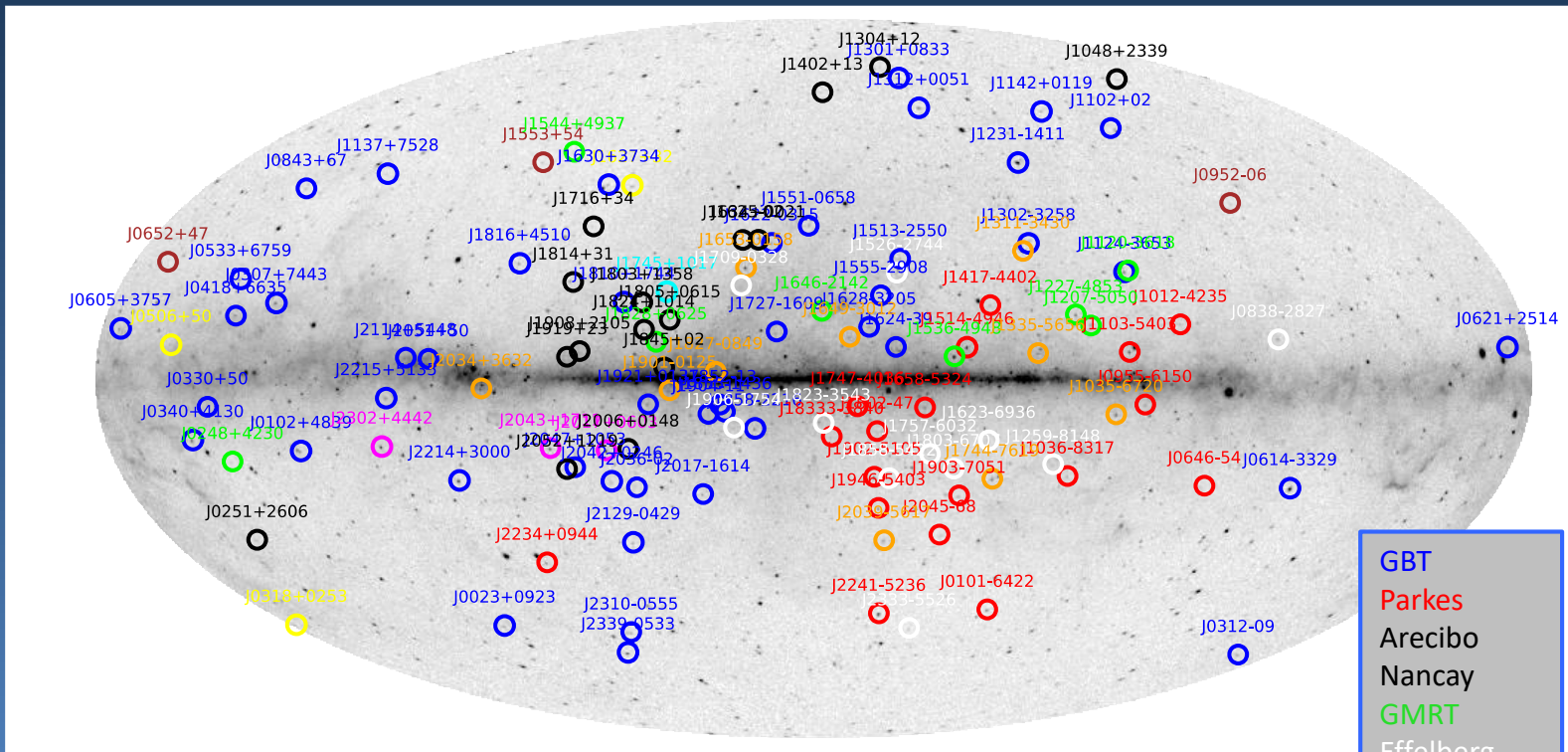
Newly discovered radio PSR J1023+0038 was accreting source FIRST J102347.67+003841.2 in 2002

Two other tMSPs and several candidates found since



MSPs discovered in Fermi unID sources

126 new radio MSPs discovered in Fermi unidentified sources!

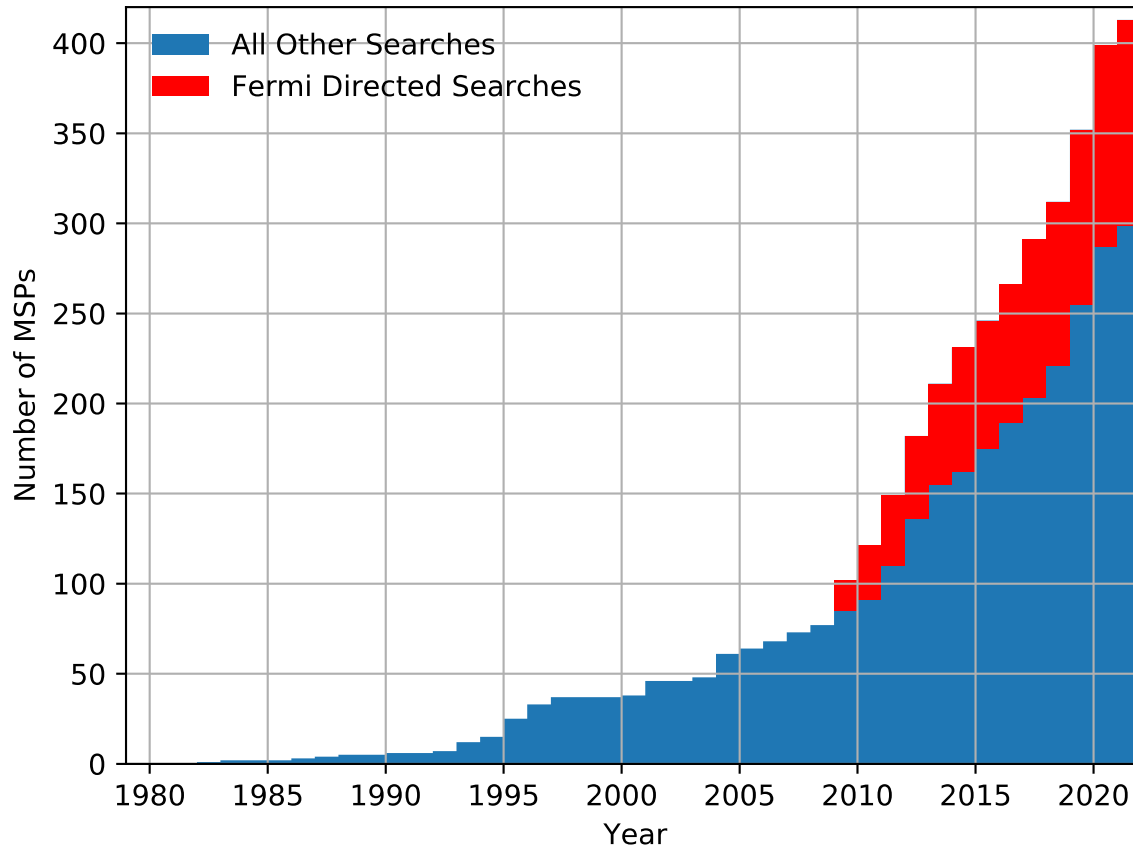


- GBT
- Parkes
- Arecibo
- Nancay
- GMRT
- Effelberg
- Fermi-LAT

95 so far with γ -ray pulsations

Credit: Paul Ray

Cumulative Number of Known Field MSPs



Gamma-ray MSPs and gravitational waves

Radio pulsar timing arrays

HUNTING GRAVITATIONAL WAVES USING PULSARS

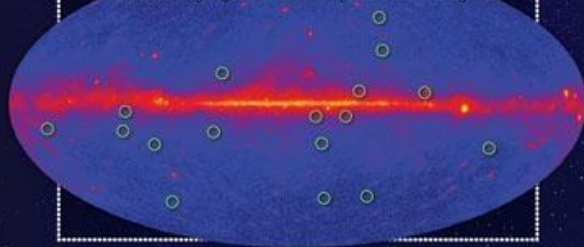
1 Gravitational waves from supermassive black-hole mergers in distant galaxies subtly shift the position of Earth.

2 Telescopes on Earth measure tiny differences in the arrival times of the radio bursts caused by the jostling.

3 Measuring the effect on an array of pulsars enhances the chance of detecting the gravitational waves.

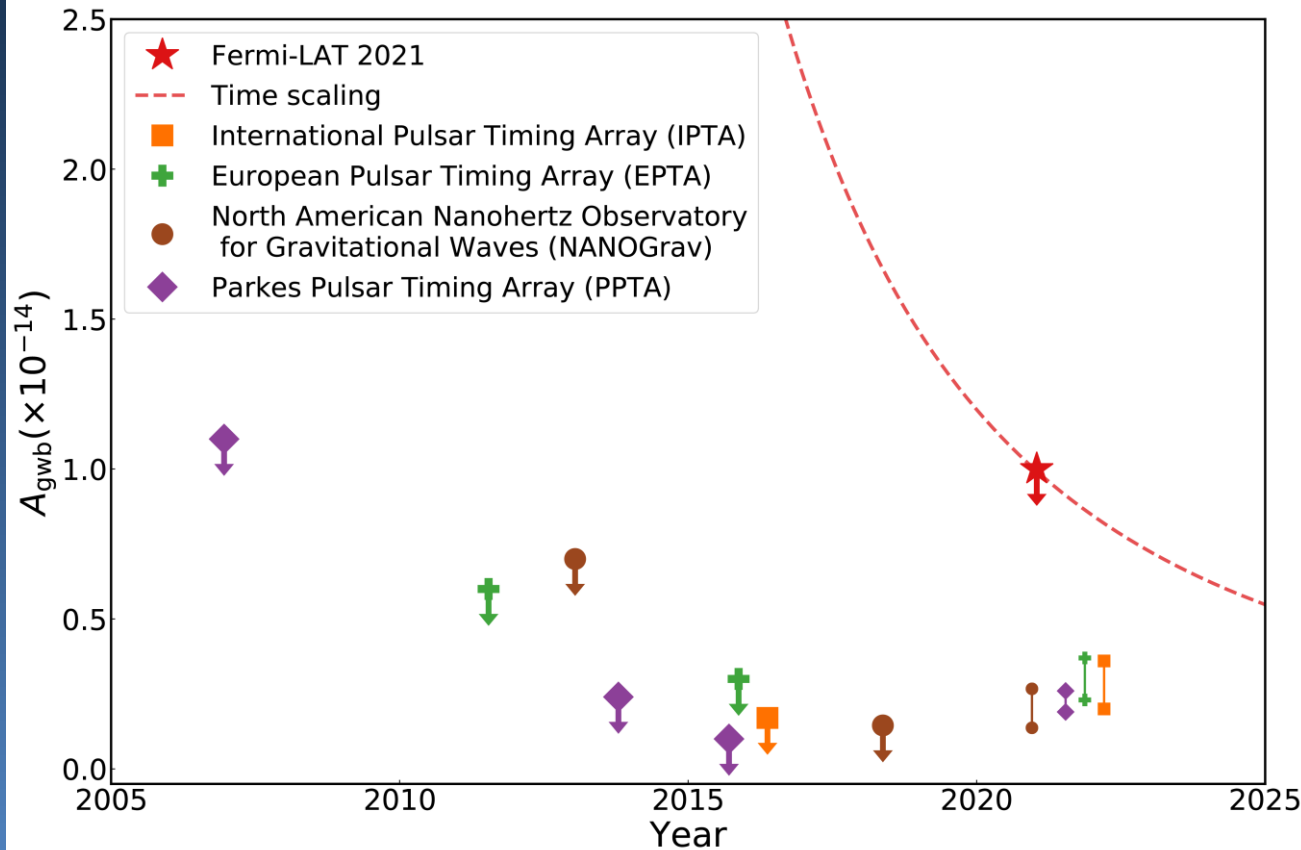
NEW MILLISECOND PULSARS

An all-sky map as seen by the Fermi Gamma-ray Space Telescope in its first year



Gamma-ray MSPs and gravitational waves

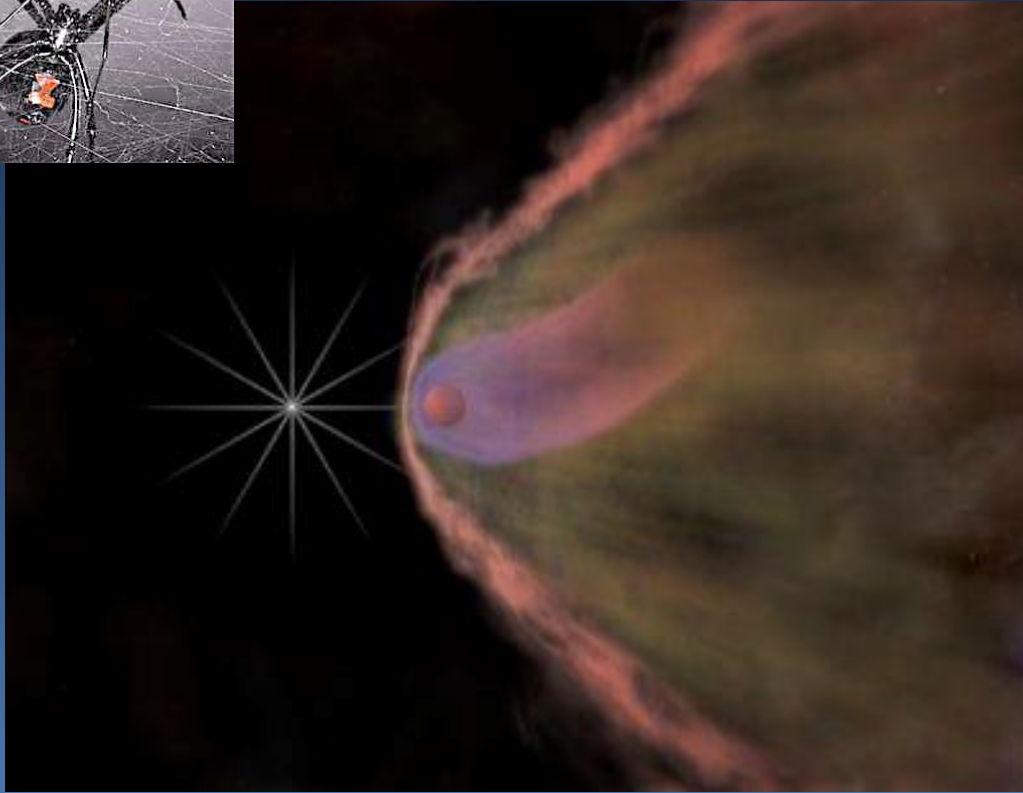
Ajello et al. (Fermi Collaboration) 2022



Gamma-ray pulsar timing array!

- 12.5 years of Fermi data
- 35 bright MSPs
- Limit on stochastic GW signal $< 10^{-14}$
- Will reach radio timing array limit in 2 years!

Spider millisecond pulsars



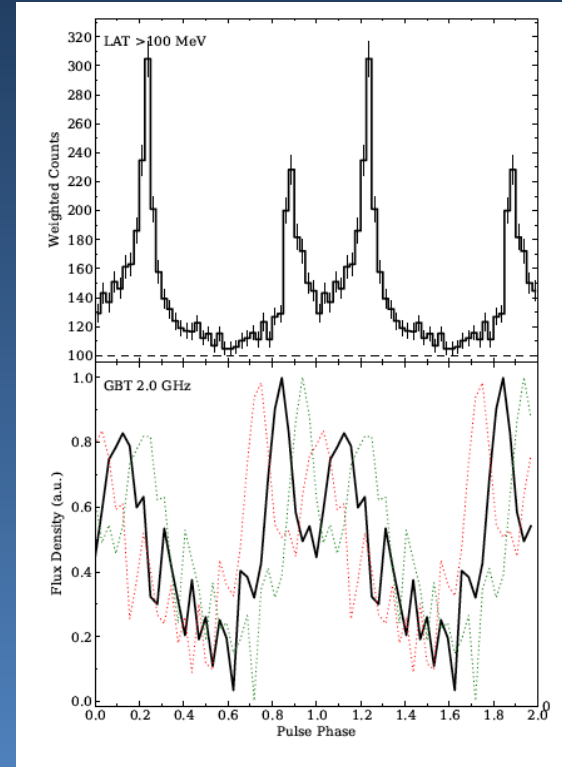
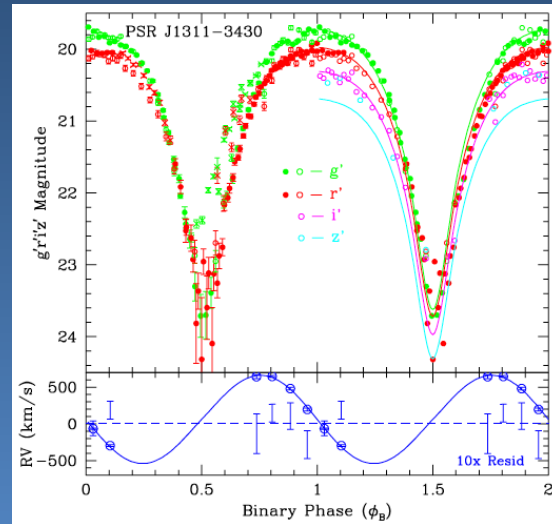
- Black Widows - MSPs with very low-mass binary companions
 - 10 – 80 Jupiter masses ($< 0.1 M_{\odot}$)
- Pulsar wind ablates companion by exciting stellar winds
- Redbacks (cousins)
 - $> 0.1 M_{\odot}$ companions

Before Fermi launch: 3 Black Widows, 1 Redback
Now: 31 Black Widows, 12 Redbacks – Total of 43!

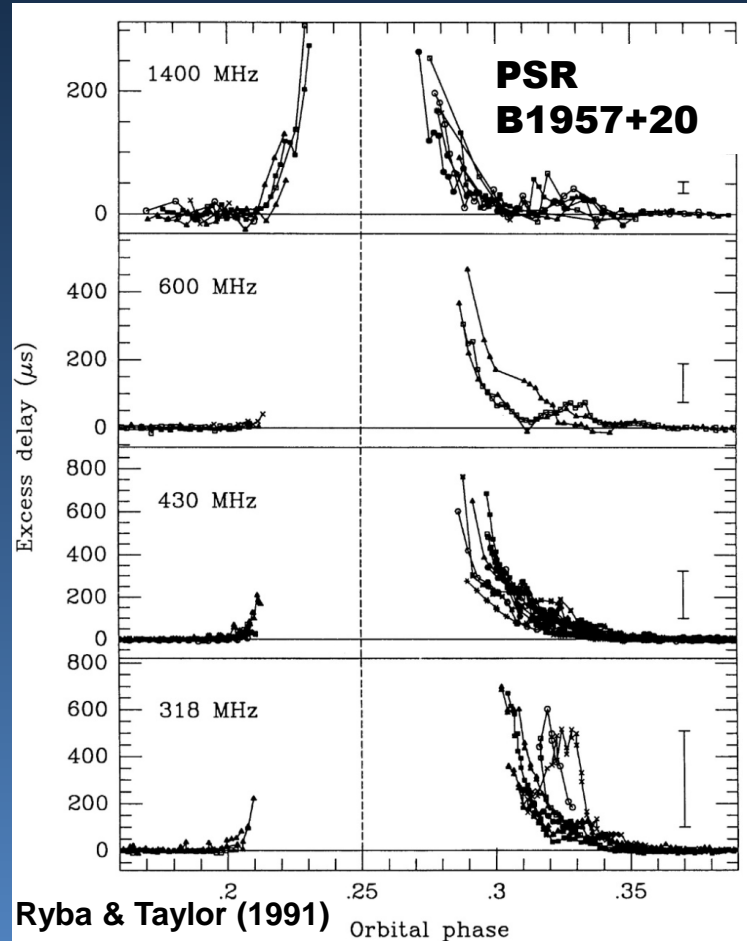


Fermi 'web' catches Black Widow

- Optical orbital modulation found in 2FGL J1311.7-3429 (Romani et al. 2012)
- First MSP J1311-3430 discovered in γ -ray blind search of 2FGL J1311.7-3429 (Pletsch et al 2012)
- But not a radio quiet pulsar! (Ray et al. 2012)
- Tiny companion ($0.008 M_{\odot}$) and smallest known orbit (1.5 hr – Earth/Sun distance!)



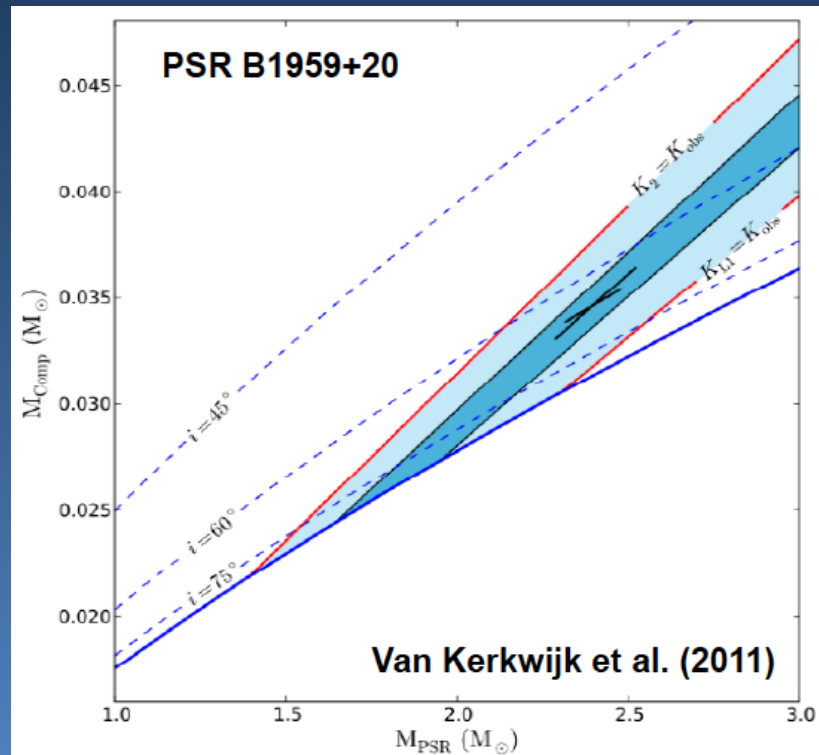
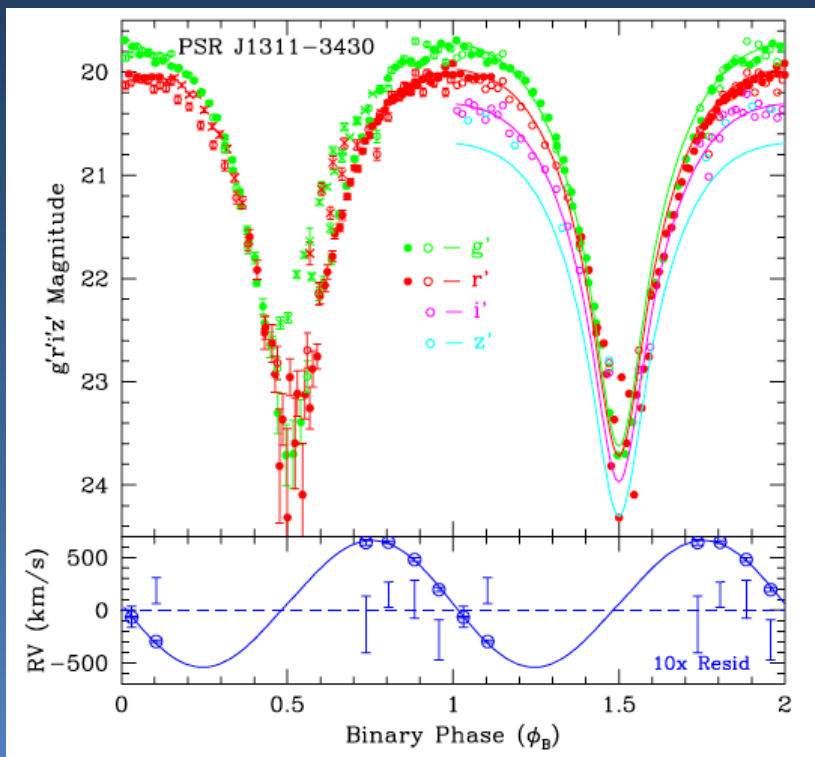
Radio properties



- Frequency-dependent radio eclipses (disappearance of radio pulses).
- Shrouding of MSP pulsed radio emission by intra-binary material.
- Phase of eclipse discriminates shock orientation.
- Asymmetry of eclipse decreases with frequency: higher frequency observations probe denser regions closer to the shock.

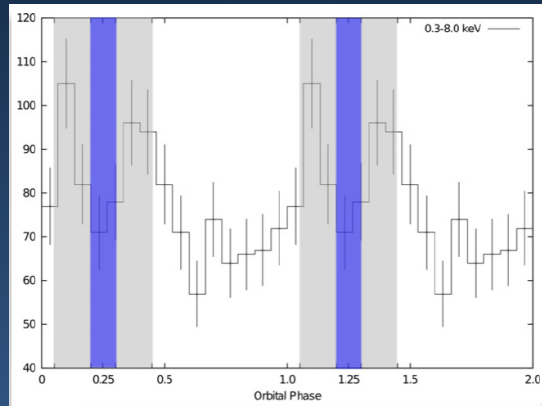
Optical observations of the stellar companion

- Optical light curve modeling can constrain orbital inclination and mass ratio
- Companion temperature as high as few times 10^4 K on heated side

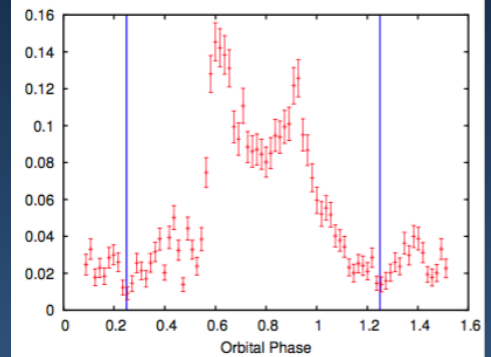


Double-peaked soft X-ray light curves

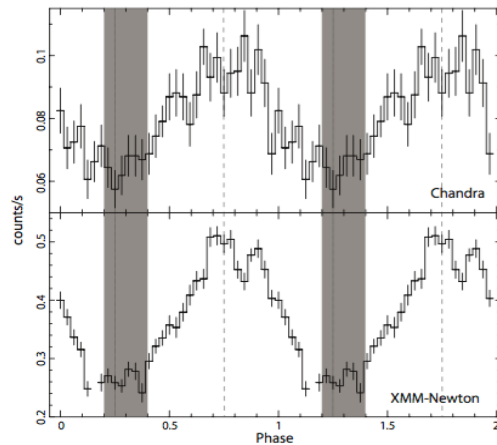
- Flux minimum around superior (BW) or inferior (RB) conjunction
- Spectral indices $\Gamma \sim 1 - 1.5$
- Synchrotron, modulated by Doppler boosting



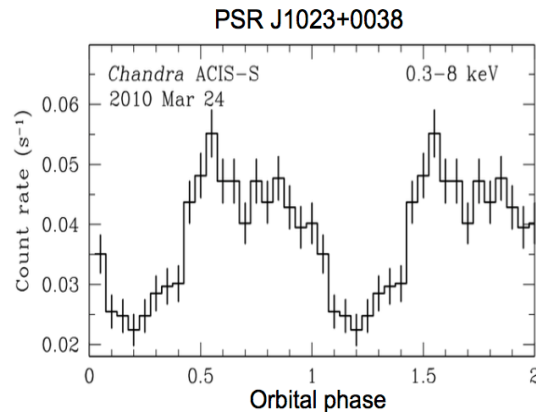
B1957+20 Huang et al. 2012



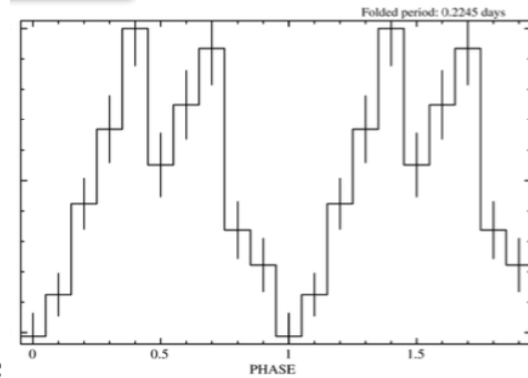
J2129-0429, Roberts et al. 2015



J1723-2837, Hui et al. 2014



J1023+0038, Archibald et al. 2010

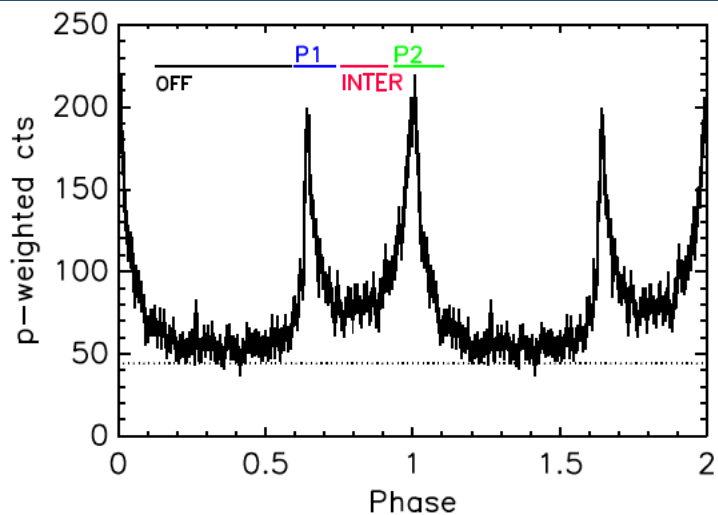


J2039-5618, Salvetti et al. 2015

Gamma-ray properties

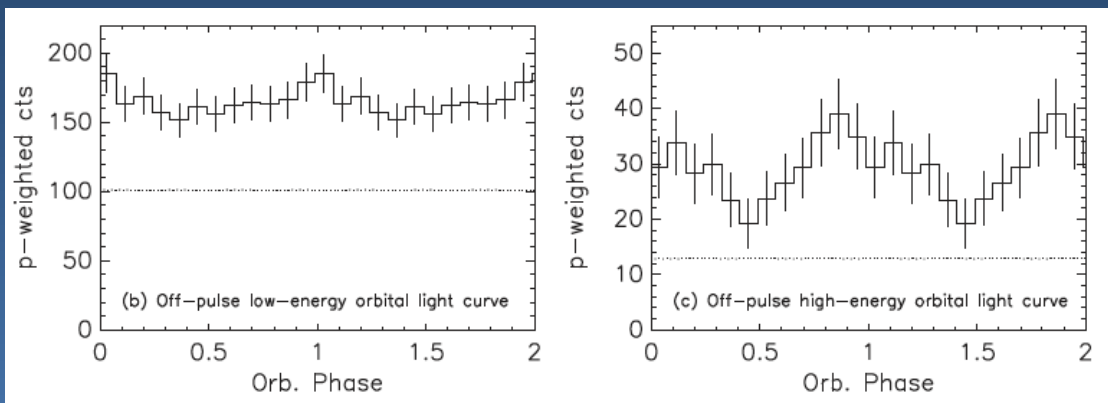
An et al. 2017

Fermi pulsar light curve



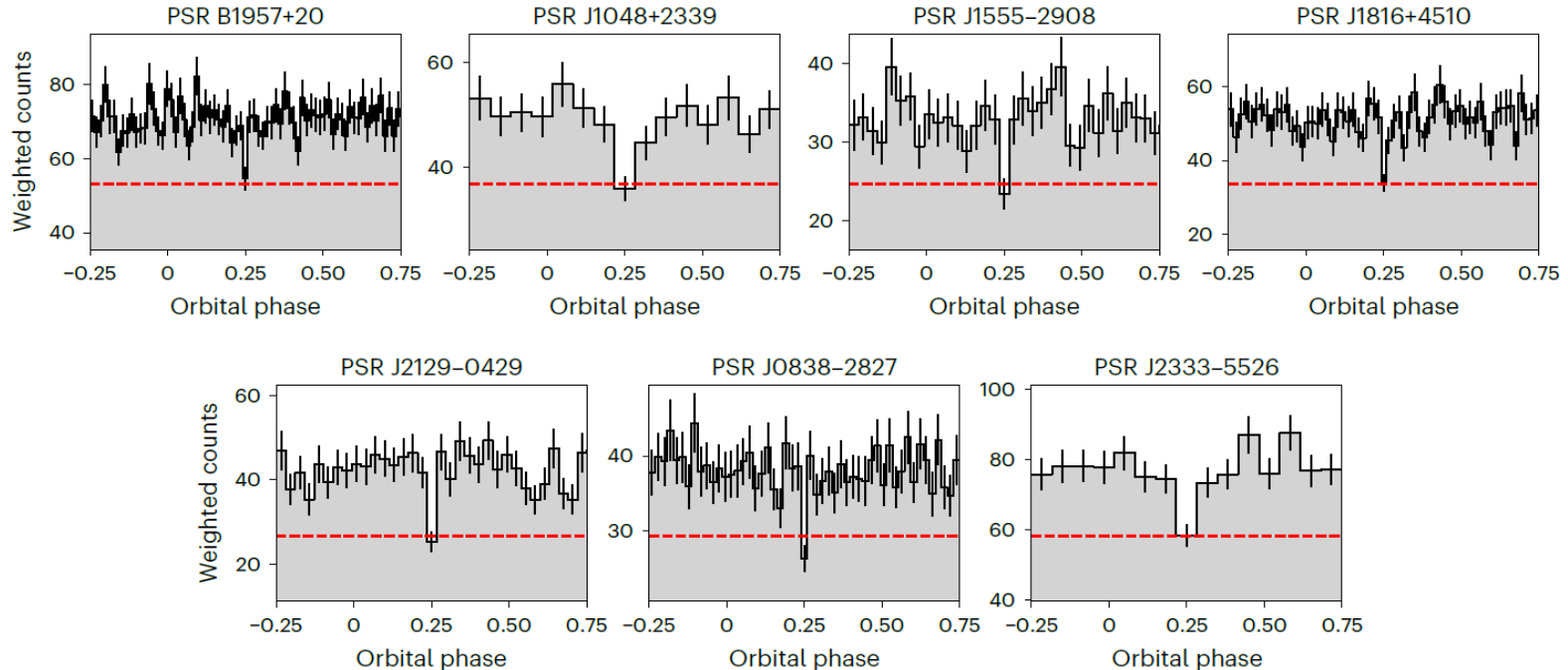
PSR J1311-3430 orbital modulation

Fermi off-pulse light curve

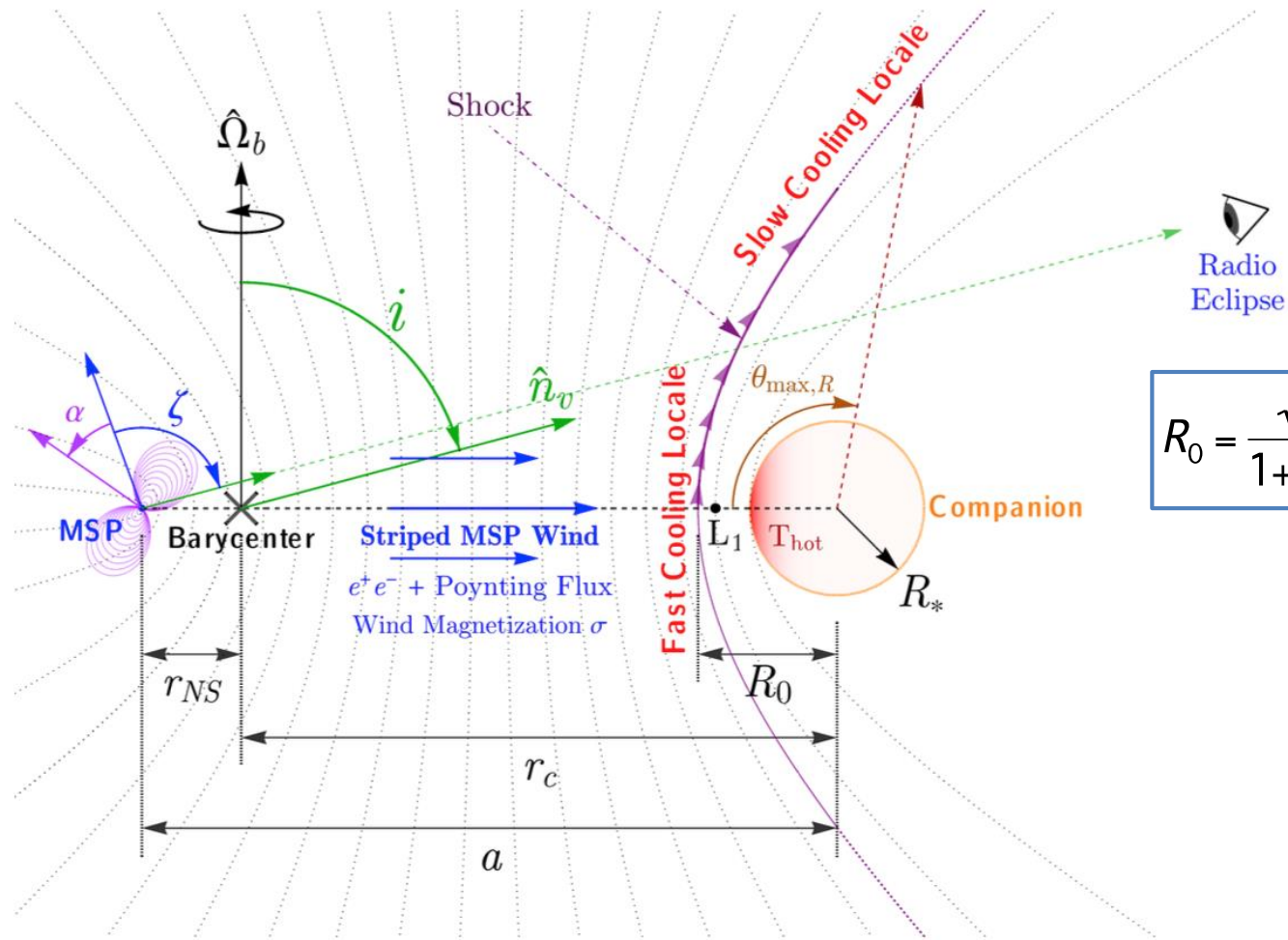


Gamma-ray eclipses

- Gamma-ray eclipses in 7 systems (out of 49), including PSR B1957+20, due to occultations by companion
- Limit i and provide robust limits on the M_{PSR} (circumventing uncertainties in optical heating model) (Clark et al. 2023)



Black widow and Redback binaries

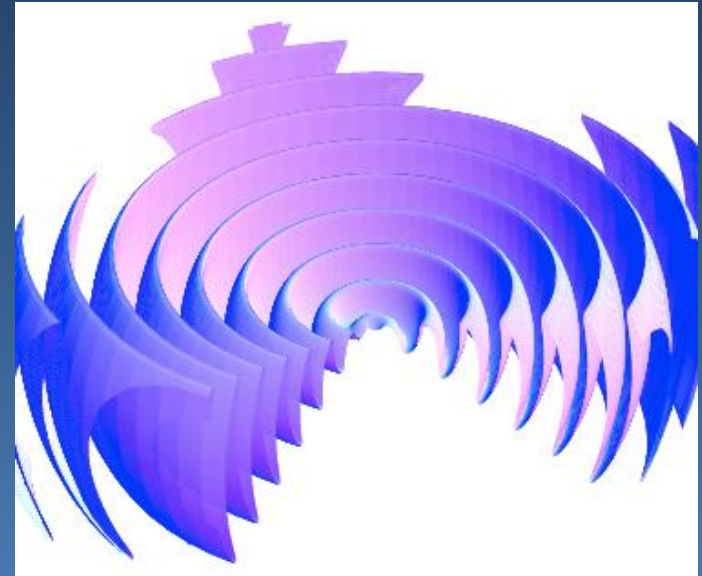
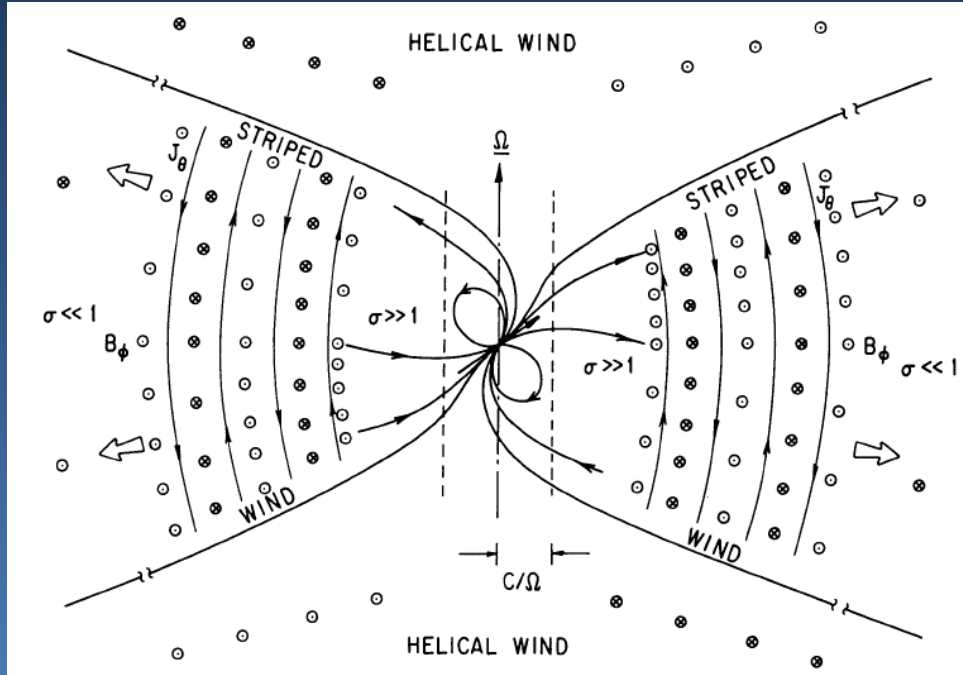


Harding & Gaisser 1990

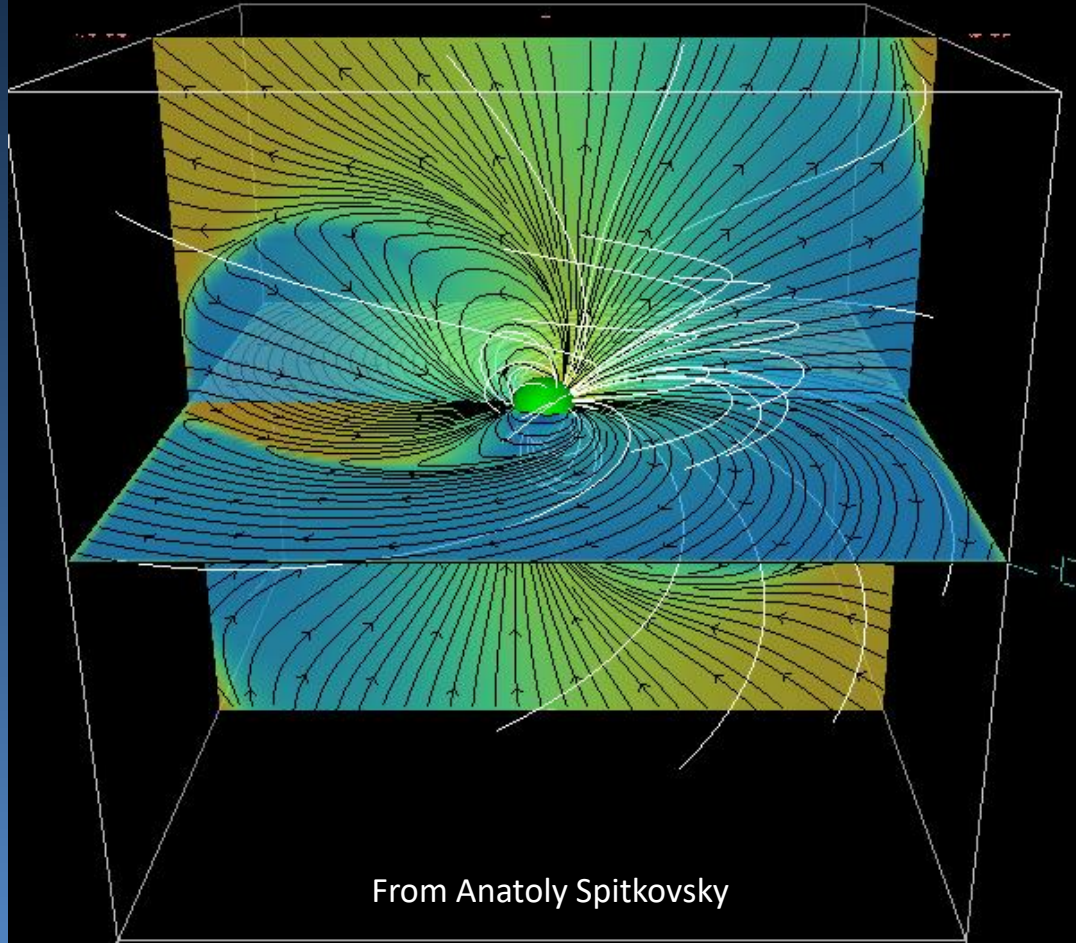
$$R_0 = \frac{\sqrt{\eta_w}}{1 + \sqrt{\eta_w}} \quad \eta_w = \frac{P_{comp}}{\dot{E}_{SD}/c}$$

If $\eta_w < 1$, shock surrounds companion
 If $\eta_w > 1$, shock surrounds the MSP

Pulsar striped wind



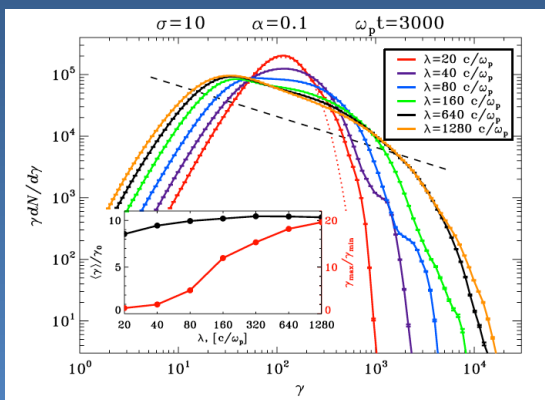
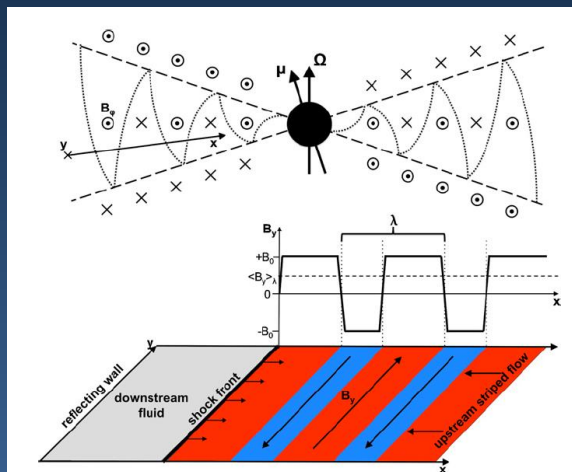
3D pulsar magnetosphere



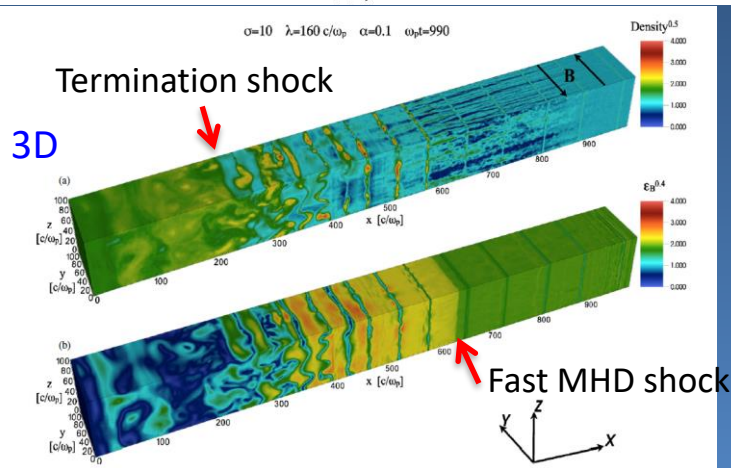
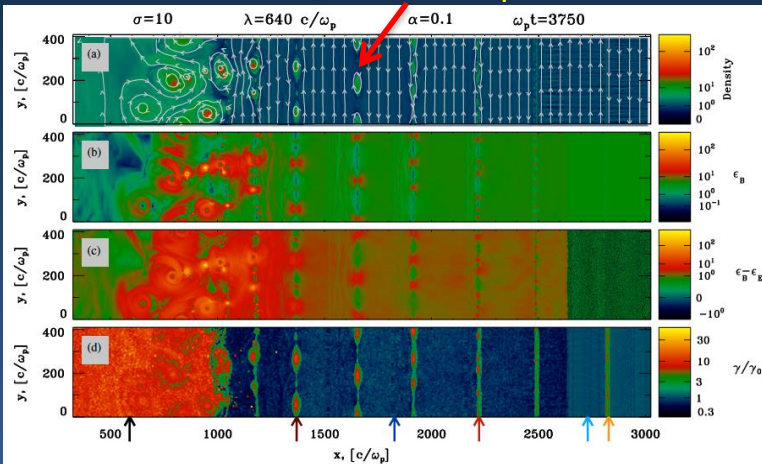
From Anatoly Spitkovsky

Shock-driven reconnection

Sironi & Spitkovsky 2011

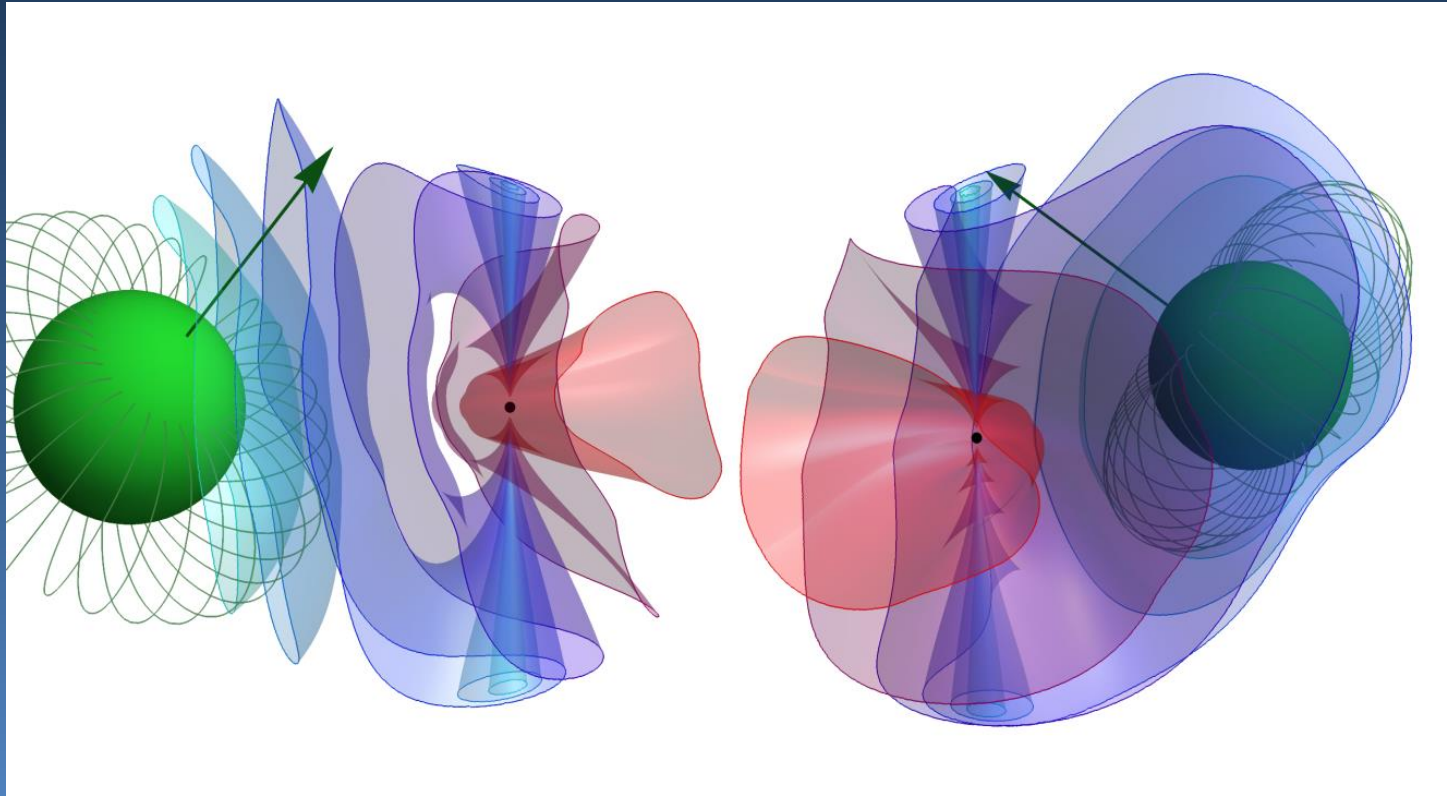


2D Particles accelerated at X-points where $E > B$



Magnetic pressure of companion

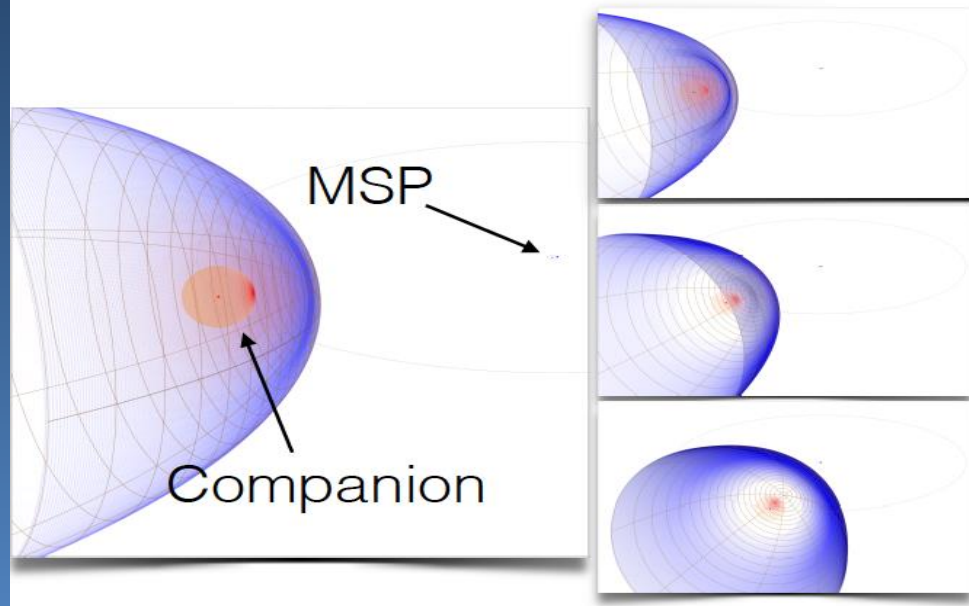
Wadiasingh et al. 2018



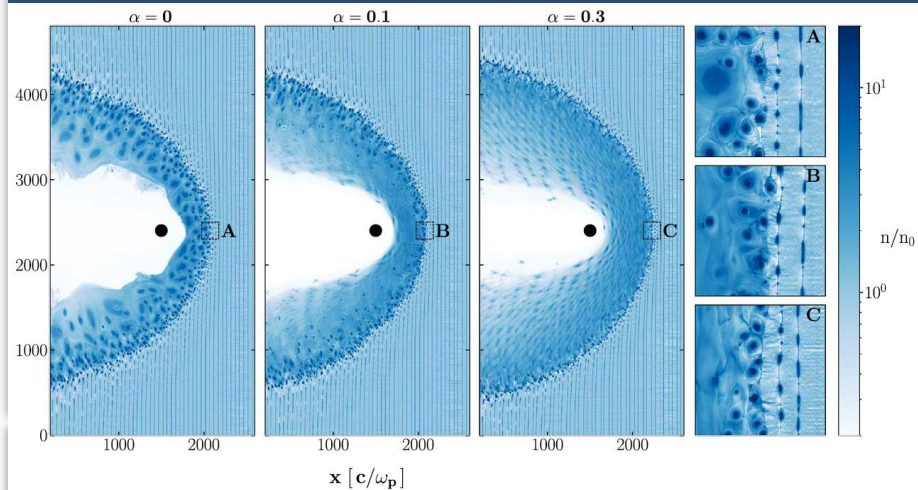
Shock geometry

Use analytic solution for shock geometry from isotropic colliding winds (Canto et al. 1996)

- Schematic B1957+20 shock *to scale*:



PIC simulations (Cortez & Sironi 2022)



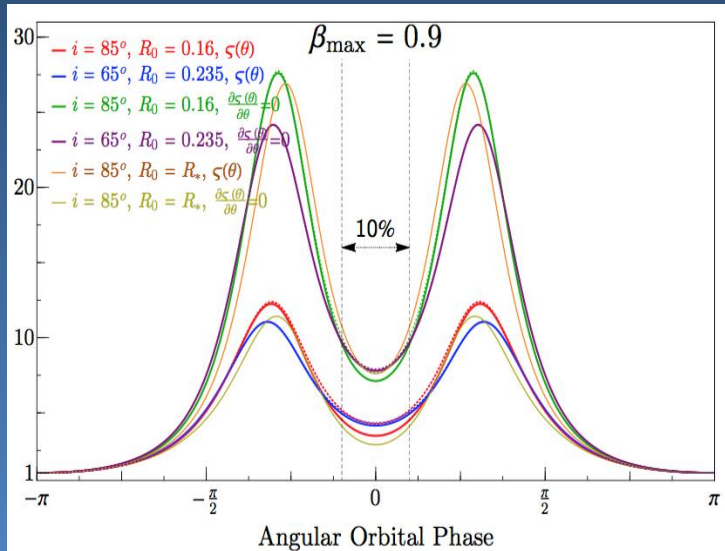
Orbitally modulated synchrotron emission

Wadiasingh et al. 2017

- Doppler boosting produces a double-peaked light curve for high bulk flow velocity centered on inferior conjunction
- Bulk flow $\beta_{\max} > 0.5$ needed for doubled-peaked light curves

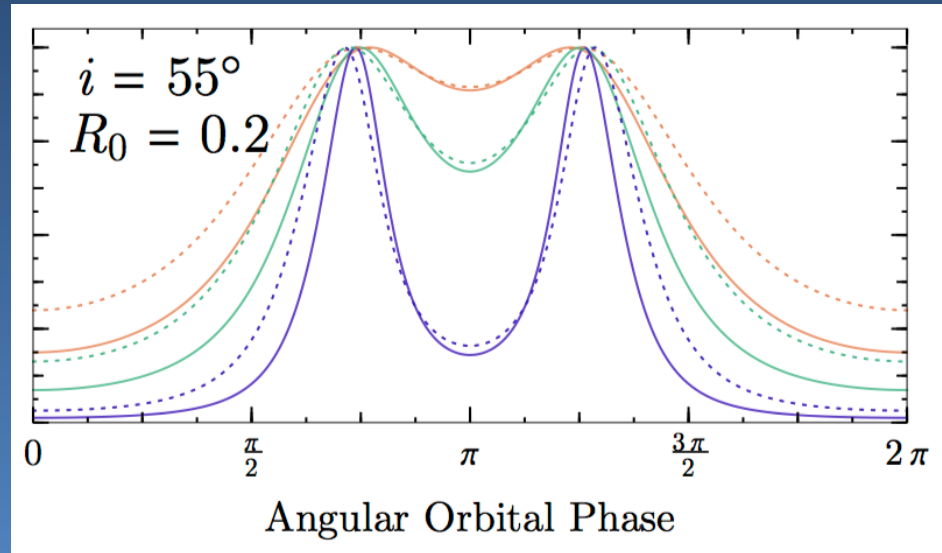
Shock surrounding companion (e.g. B1957+20)

Light curve centered on superior conjunction

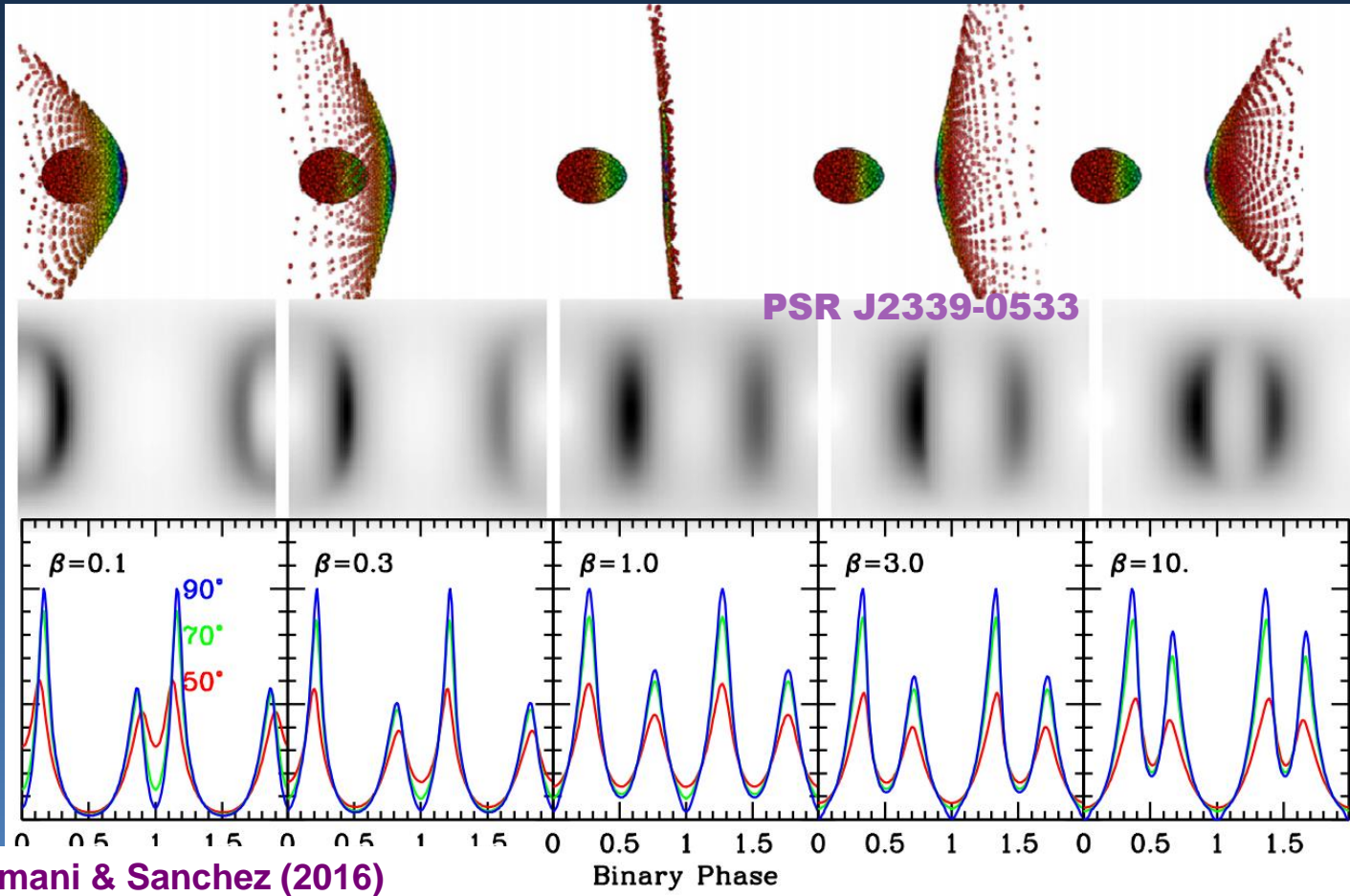


Shock surrounding pulsar (e.g. J1023+0038)

Light curve is centered on inferior conjunction

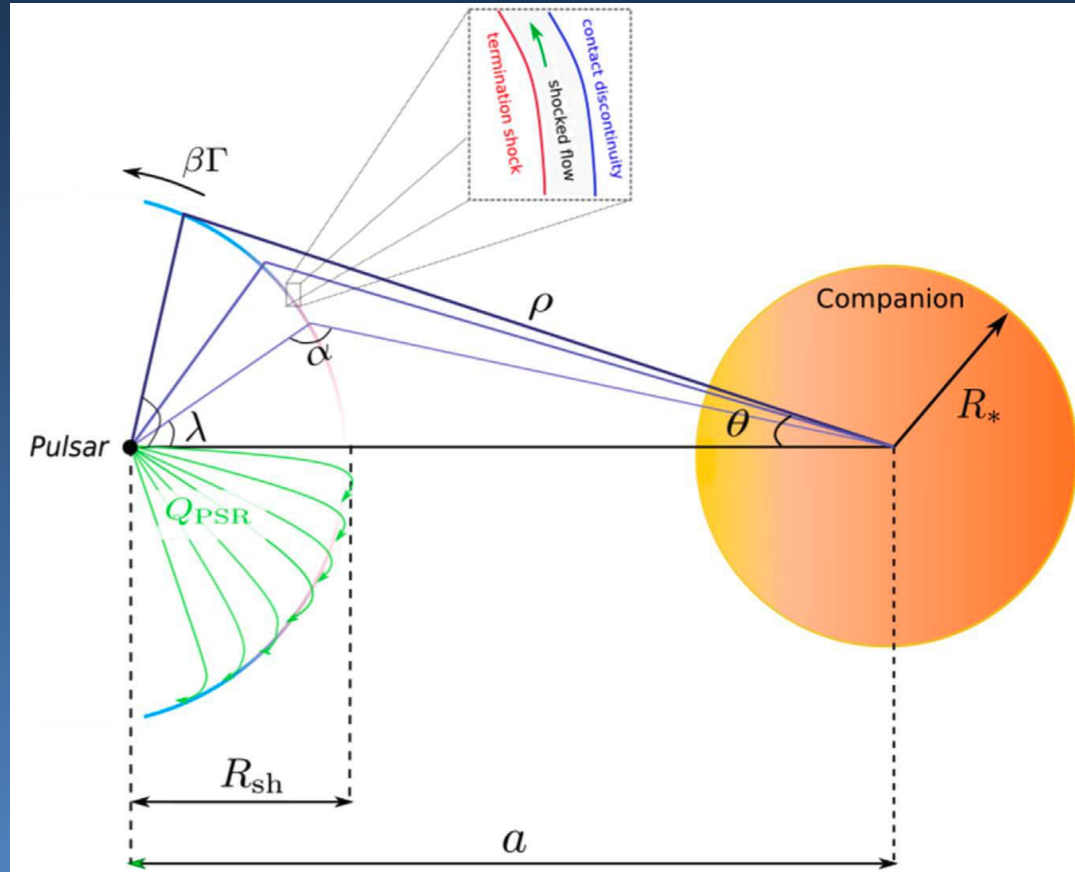


Intrabinary shock emission

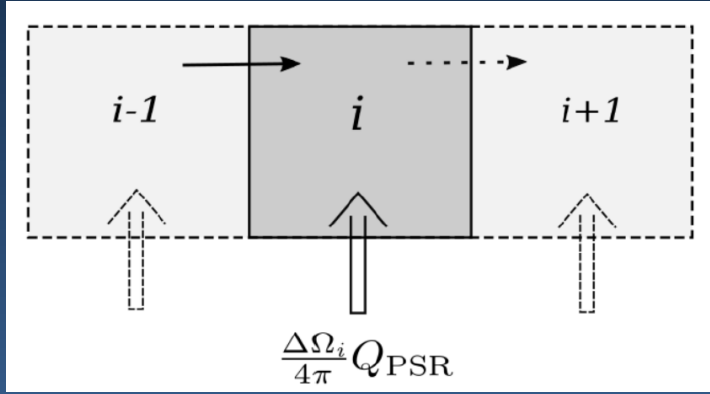


Shock emission model

Van der Merwe et al. 2020



Particle transport



$$Q_{\text{PSR}}(E_e) = Q_0 E_e^{-\Gamma} \exp\left(-\frac{E_e}{E_{\text{cut}}}\right)$$

$$\int_{\gamma_{e,\min}}^{\infty} Q_{\text{PSR}} d\gamma_e = (M_{\pm} + 1) \dot{N}_{\text{GJ}},$$

$$m_e c^2 \int_{\gamma_{e,\min}}^{\infty} \gamma_e Q_{\text{PSR}} d\gamma_e = \eta_p \dot{E}_{\text{rot}},$$

$$\frac{\partial N_e}{\partial t} = -\vec{V} \cdot (\vec{\nabla} N_e) + \kappa(\gamma_e) \nabla^2 N_e + \frac{\partial}{\partial \gamma_e} (\dot{\gamma}_{e,\text{tot}} N_e) - (\vec{\nabla} \cdot \vec{V}) N_e + Q$$

$$0 = -\frac{N_{e,i}}{\tau_{\text{ad},i}} - \frac{N_{e,i}}{\tau_{\text{diff},i}} - \frac{N_{e,i}}{\tau_{1,i}} - \frac{N_{e,i}}{\tau_{2,i}} - \frac{N_{e,i}}{\tau_{\text{rad},i}} + Q_i$$

$$Q_i = \frac{1}{t_{\text{diff}}} \frac{dN_{e,i-1}}{dE_e} + \frac{1}{2} (\cos \lambda_i - \cos \lambda_{i+1}) Q_{\text{PSR}}, \quad i > 1$$

Maximum acceleration energy

“Hillas” criterion – $R_{\text{sh}} = r_g$

$$\gamma_{e, \text{max}}^{\text{H}} \approx \frac{eR_{\text{sh}}B_{\text{sh}}}{m_e c^2} \sim 2 \times 10^8 \left(\frac{R_{\text{sh}}}{10^{10} \text{ cm}} \right) \left(\frac{B_{\text{sh}}}{10 \text{ G}} \right)$$

Polar cap voltage drop

$$\gamma_{e, \text{max}}^{\text{P}} = \frac{e\Phi_{\text{open}}}{m_e c^2} \sim 5 \times 10^8 \left(\frac{P}{5 \times 10^{-3} \text{ s}} \right)^{-2} \left(\frac{R_{\text{PSR}}}{10^6 \text{ cm}} \right)^3 \left(\frac{B_{\text{PSR}}}{10^9 \text{ G}} \right)$$

Synchrotron loss-limited diffusive shock acceleration

$$\gamma_{e, \text{max}}^{\text{acc}} = \frac{3}{2} \sqrt{\frac{\epsilon_{\text{acc}} B_{\text{cr}}}{\alpha_f B_{\text{sh}}}} \sim 4 \times 10^7 \epsilon_{\text{acc}}^{1/2} \left(\frac{B_{\text{sh}}}{10 \text{ G}} \right)^{-1/2}$$

$$\epsilon_{\text{acc}} \equiv r_g / \lambda(\gamma_e) \leq 1$$

Reconnection in striped wind

$$\gamma_{e, \text{max}}^{\text{R}} = \gamma_0 \sigma_{\text{sh}} \approx 6 \times 10^3 \left(\frac{B_{\text{sh}}}{10 \text{ G}} \right) P_{\text{ms}} \gamma_0 / \kappa$$

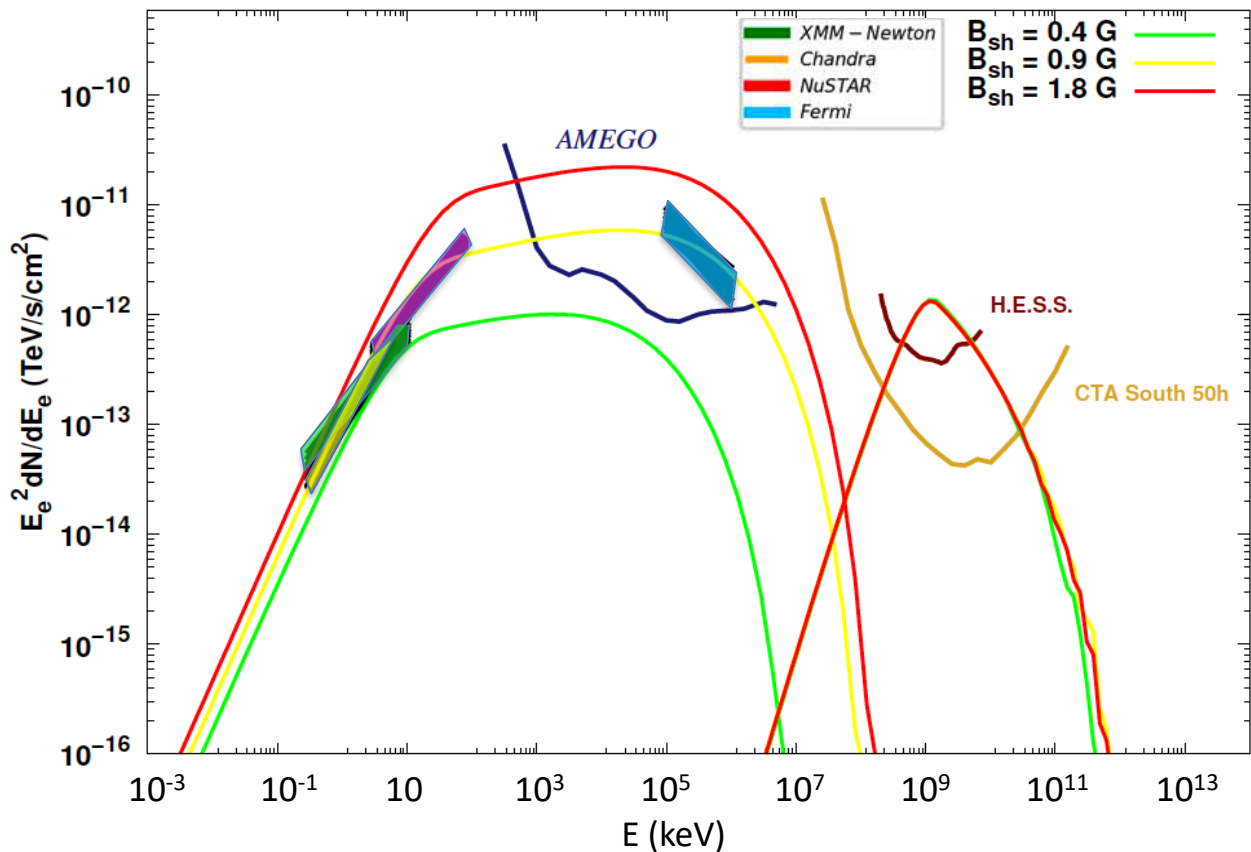
Model parameters

| Parameters | Symbols | J1311-3430 | J1311-3430 | J1723-2837 | J1959+2048 | J2339-0335 |
|--|---------------------------|------------|------------|------------|------------|--------------|
| | | Quiescent | Flaring | | | |
| | | Values | | | | |
| Pulsar mass | M_{psr} (M_{\odot}) | 2.0 | 2.0 | 2.0 | 2.0 | 2.16 |
| Pulsar radius | R_{NS} (cm) | 1.0e6 | 1.0e6 | 1.0e6 | 1.0e6 | 1.0e6 |
| Orbital period | P_b (hr) | 1.56 | 1.56 | 14.8 | 9.17 | 4.60 |
| Mass ratio | q | 180 | 180 | 3.5 | 70 | 18.2 |
| Shock radius | R_{sh} (units of a) | 0.5 | 0.4 | 0.3 | 0.4 | 0.3 |
| B-field at the shock | B_{sh} (G) | 1.3 | 1.2 | 0.8 | 1.9 | 0.6 |
| Companion Temperature | T_{comp} (K) | 12000 | 45000 | 6000 | 8500 | 6000 |
| Pair multiplicity | M_{pair} | 1000 | 5000 | 1000 | 8000 | 500 |
| Maximum particle conversion efficiency | $\eta_{p,max}$ | 0.9 | 1.0 | 1.5 | 0.9 | 0.7 |
| Pulsar period | P (ms) | 2.56 | 2.56 | 1.86 | 1.60 | 2.88 |
| Pulsar period derivative | \dot{P} (s/s) | 2.1e-20 | 2.1e-20 | 7.6e-21 | 1.7e-20 | 1.4e-20 |
| Index of injected spectrum | Γ | 1.8 | 1.6 | 2.6 | 2.5 | 1.9 |
| Distance | d (kpc) | 1.40 | 1.40 | 0.72 | 1.73 | 1.10 → 0.45! |
| Bulk flow momentum | $\beta_{\Gamma,max}$ | 4.0 | 10 | 6.0 | 3.0 | 12.0 |
| Inclination angle | i (degrees) | 60 | 60 | 40 | 65 | 54 |

PSR J1723-2873 (RB)

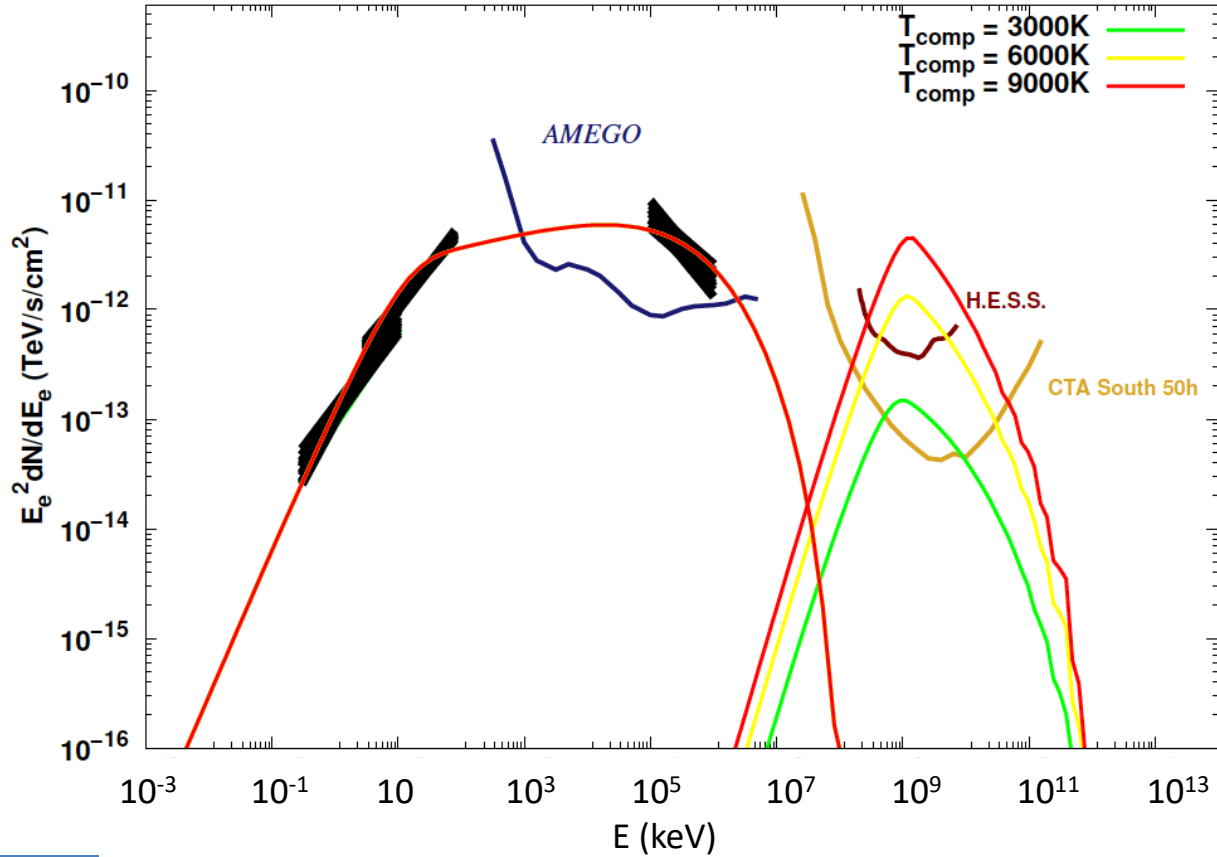
Van der Merwe et al. 2020

Dependence on B at shock

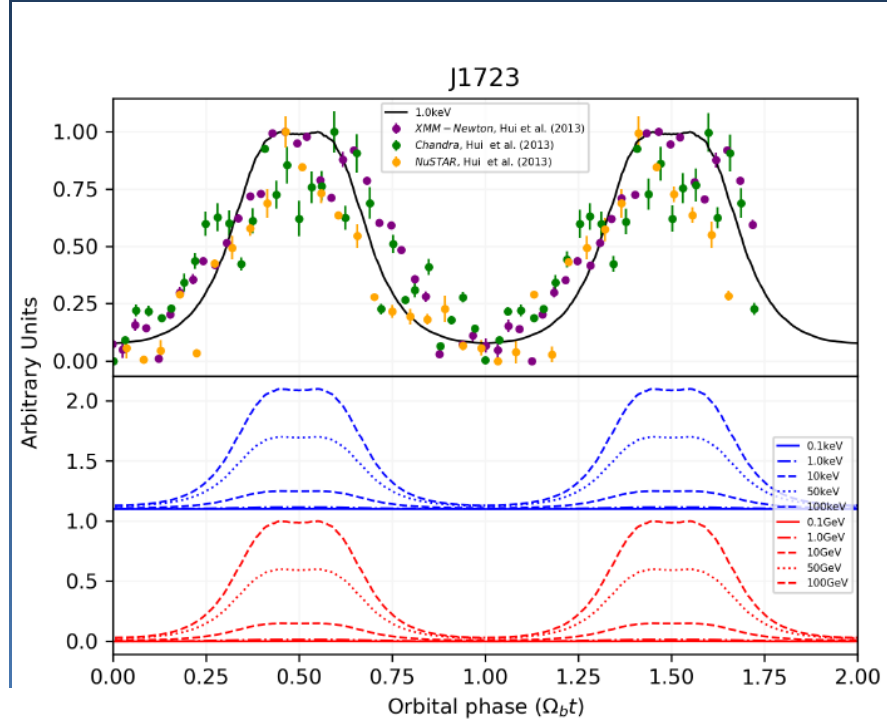
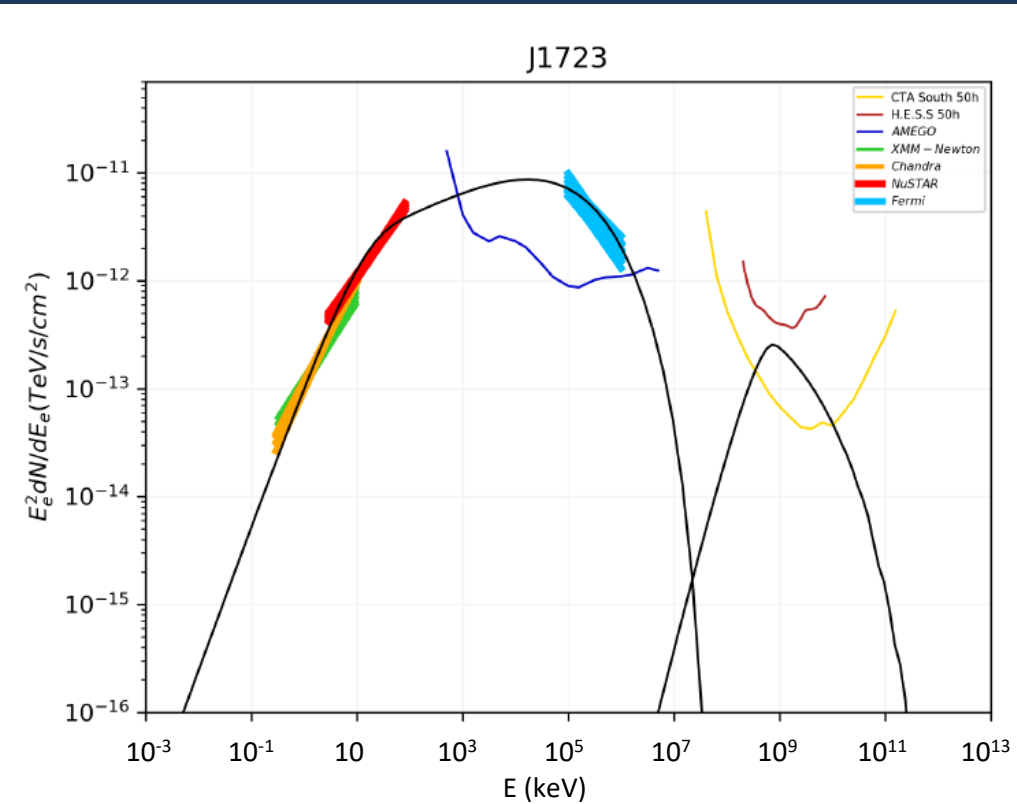


PSR J1723-2873 (RB)

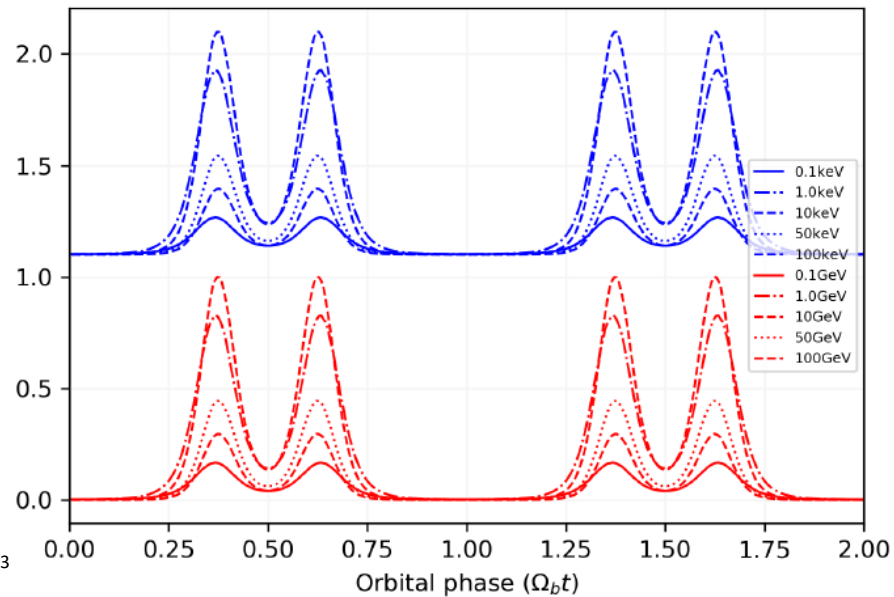
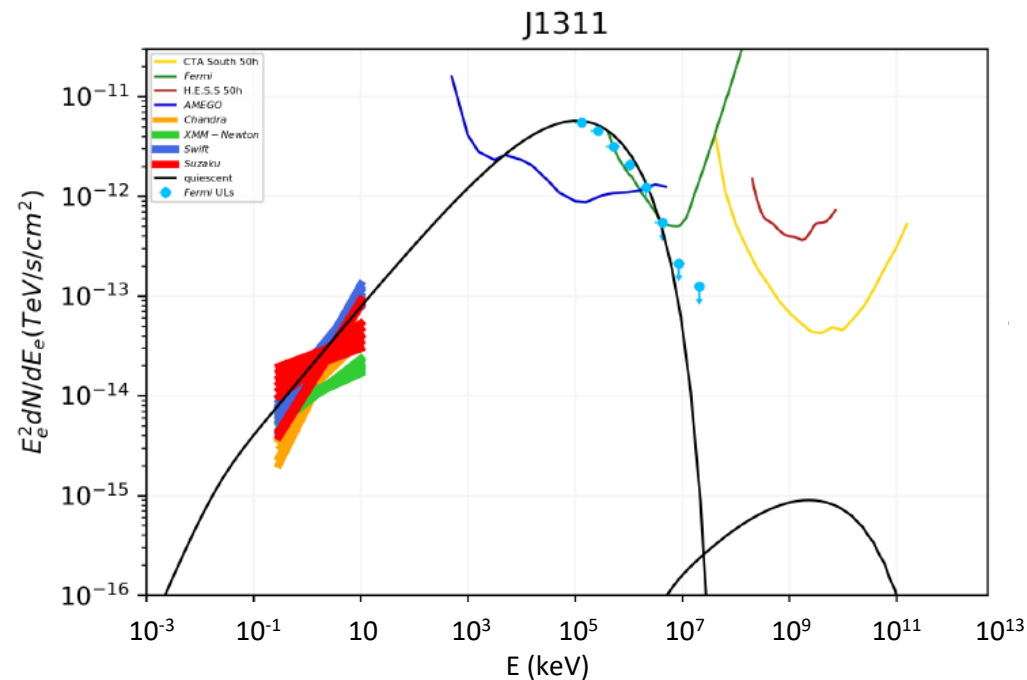
Dependence on temperature of companion



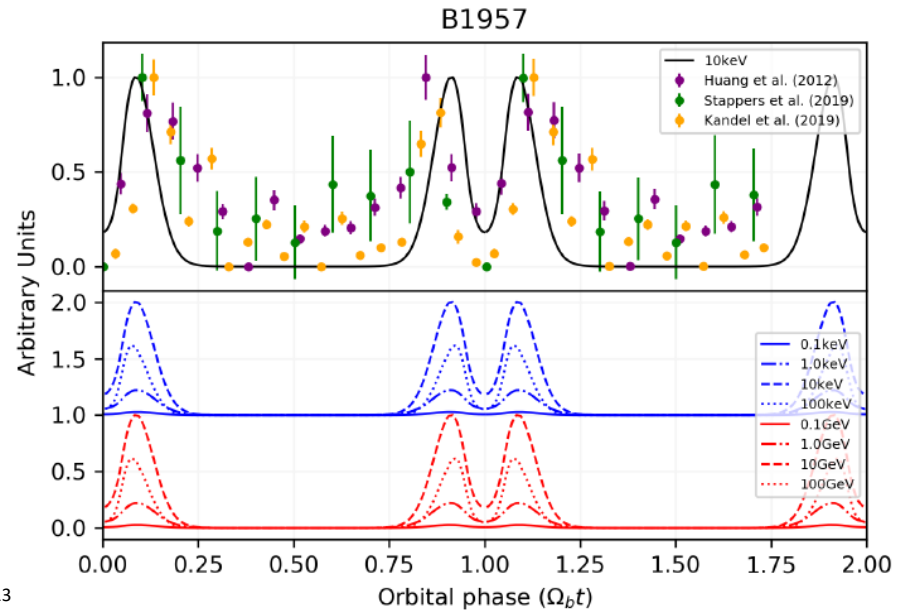
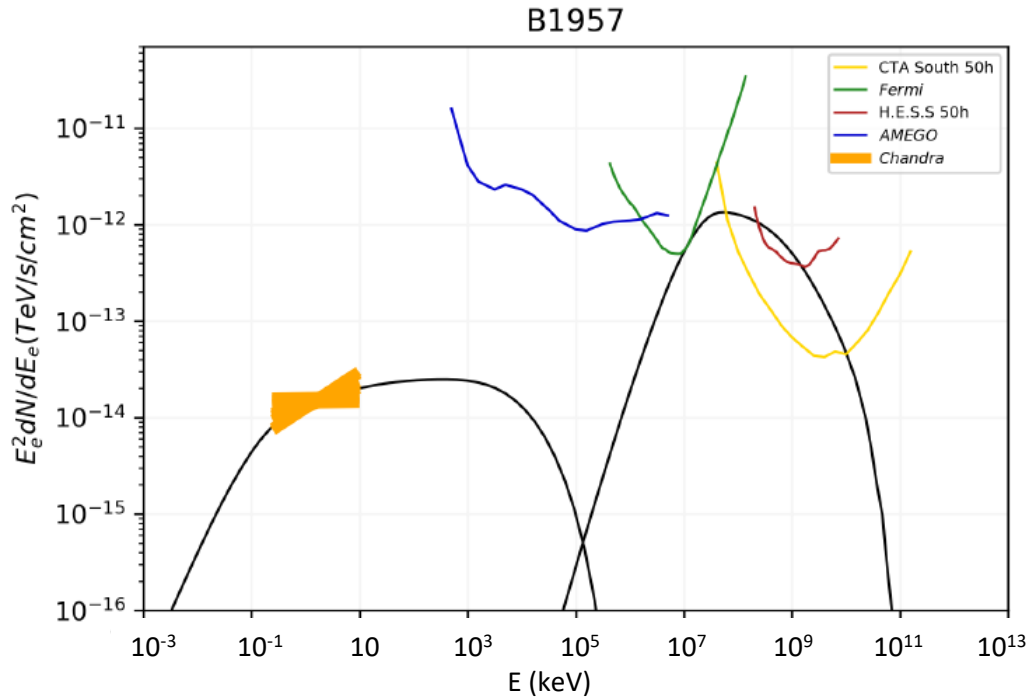
PSR J1723-2873 (RB)



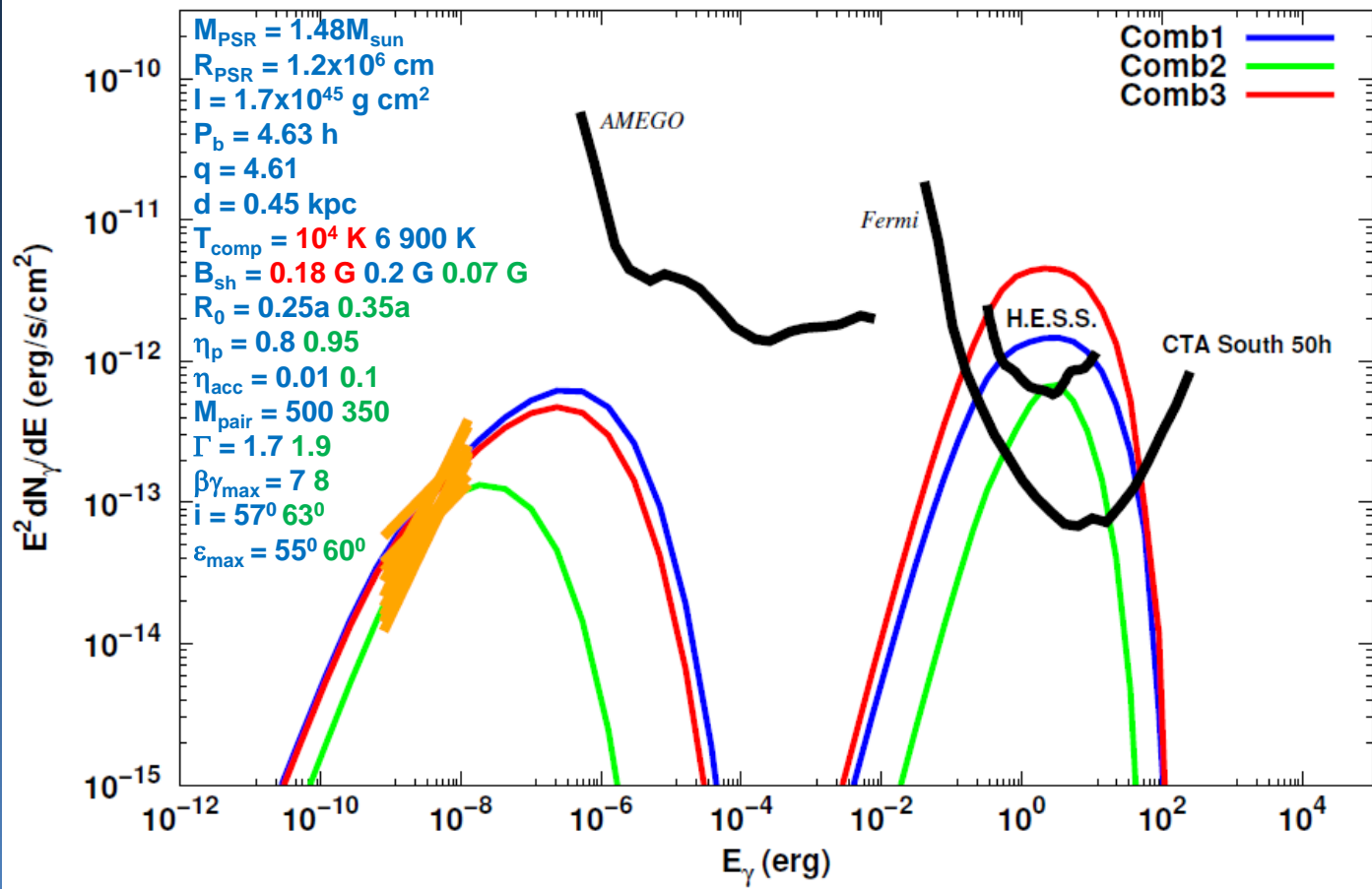
PSR J1311-3430 (BW)



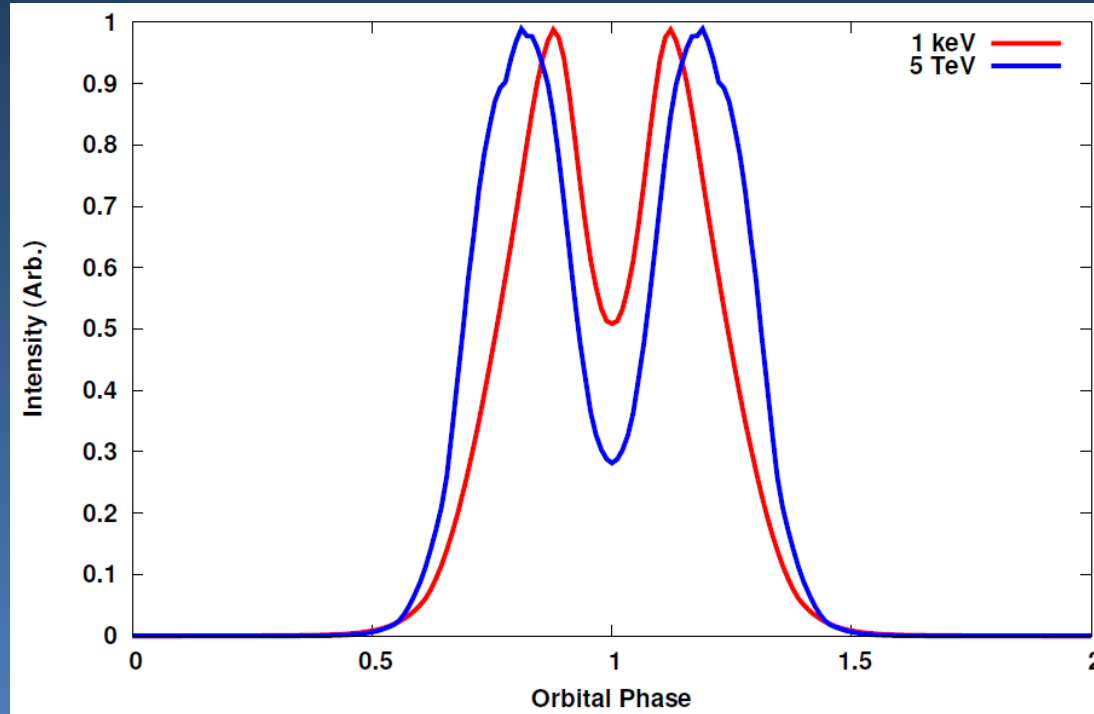
PSR B1957+20 (BW)



PSR J2339-0533 (RB)



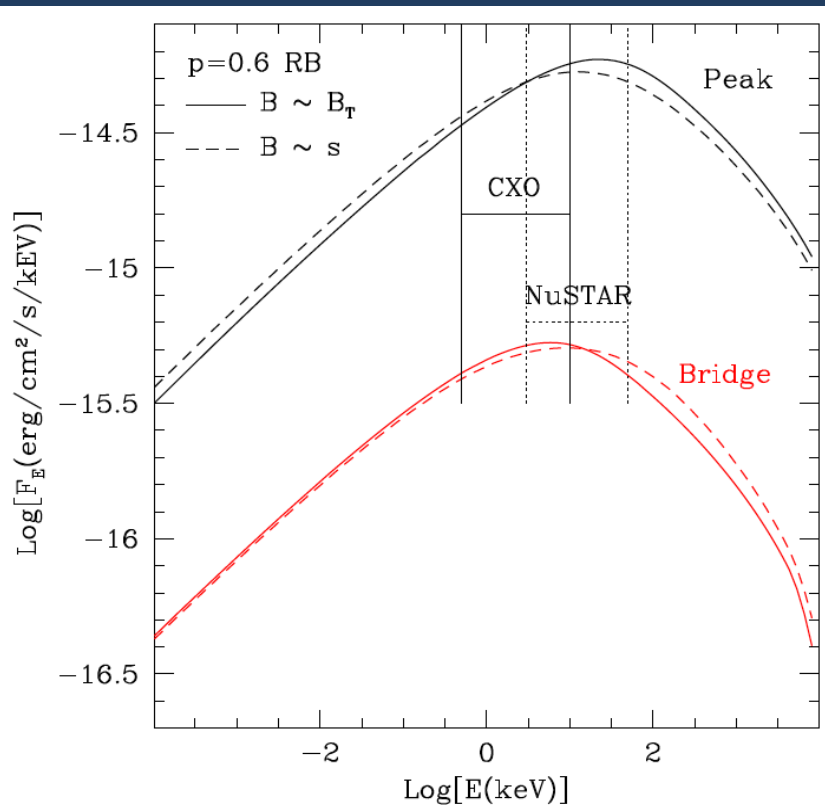
PSR J2339-0533 (RB)



What is the shock acceleration mechanism?

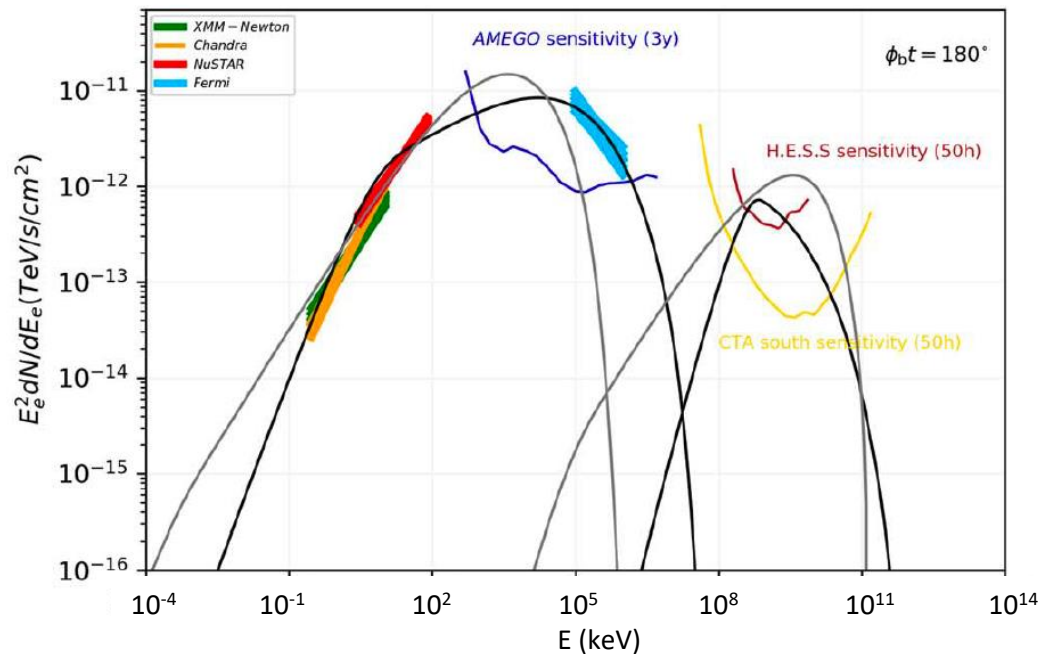
Reconnection? (Kandel, Romani & An 2019)

$$\gamma_{\max} \sim \sigma_w \gamma_w \sim 10^4$$



Diffusive shock acceleration? (Van der Merwe 2020)

$$\gamma_{\max} \sim 4 \times 10^7 \epsilon_{\text{acc}}^{1/2} \left(\frac{B_{\text{sh}}}{10 \text{ G}} \right)^{-1/2}$$



What is the shock acceleration mechanism?

Reconnection

Particle spectrum as hard as $p \sim 1.0$

Photon SR index $\alpha = -(p + 1) / 2 \sim -1$

Diffusive shock acceleration

Particle spectrum $p \sim 2.0$ for compression ratio $r \sim 4$

But if injected spectrum is $p = p_0 < 2.0$, accelerated particle spectrum will be $p = p_0$
(Jones & Ellison 1991)

MSP pair spectra have $p_0 \sim 1.5$

Photon SR index $\alpha \sim -1.25$

Summary

- A large fraction of millisecond pulsars discovered by Fermi – many are redbacks and black widows
- Doppler boosting of synchrotron emission produces double-peaked light curve seen in black widow and redback binaries
- Intrabinary shock acceleration mechanism not resolved:
 - Shock-driven reconnection – $\gamma_e^{\max} \sim 10^{4-5}$
 - DSA - $\gamma_e^{\max} \sim \text{few } 10^6$
 - Proton acceleration??
- Detection of TeV emission from spiders will support DSA model